Molecular Pharmacology Fast Forward. Published on July 24, 2012 as doi: 10.1124/mol.112.080317

MOL #80317

The intrinsically low open probability of α7 nAChR can be overcome by positive allosteric modulation and serum factors leading to the generation of excitotoxic currents at physiological temperatures.

Dustin K. Williams, Can Peng, Matthew R. Kimbrell, and Roger L. Papke

Dept. of Pharmacology and Therapeutics, University of Florida, College of Medicine, Gainesville, Florida, USA (DKW, CP, MRK, RLP)

Molecular Pharmacology Fast Forward. Published on July 24, 2012 as DOI: 10.1124/mol.112.080317
This article has not been copyedited and formatted. The final version may differ from this version.

MOL #80317

Running Title page

Running title: Factors regulating cytotoxicity of α7 activation

*To whom correspondence should be addressed:
Name: Roger L. Papke
Phone: 352-392-4712
Fax: 352-392-9696
E-mail: rlpapke@ufl.edu
Address: Department of Pharmacology and Therapeutics
University of Florida
P.O. Box 100267
Gainesville, FL 32610-0267

Number of text pages:.....35
Number of tables:.....2
Number of figures:.....10
Number of references:.....57
Number of words in Abstract:.....250
Number of words in Introduction: 676
Number of words in Discussion:.....1516

Abbreviations:

ACh, acetylcholine; α-btx, alpha-bungarotoxin; BSA, bovine serum albumin; D_i, PNU-120596-insensitive desensitization; DMEM, Dulbecco's modified eagle medium; FBS, fetal bovine serum; DMSO, Dimethyl sulfoxide; HBSS, Hank's balanced saline solution; MLA, methyllycaconitine; nAChR, nicotinic acetylcholine receptor; PAM, positive allosteric modulator; P_{open}, probability of ion channel being open; RT-PCR, reverse-transcription polymerase chain reaction; thapsi, thapsigargin

Structure-based names:

5HI, 5-hydroxyindole; GTS-21, 3-(2,4-dimethoxybenzylidene)anabaseine; NS-1738, *N*-(5-chloro-2-hydroxyphenyl)-*N*'-[2-chloro-5-(trifluoromethyl)phenyl]urea; NS-6740, (1,4-diazabicyclo[3.2.2]nonan-4-yl(5-(3-(trifluoromethyl)phenyl)furan-2-yl)methanone; PNU-120596, *N*-(5-chloro-2,4-dimethoxyphenyl)-*N*'-(5-methyl-3-isoxazolyl)-urea; SB-206553, 3,5-dihydro-5-methyl-*N*-3-pyridinylbenzo[1,2-*b*:4,5-*b*']dipyrrole-1(2*H*)-carboxamide hydrochloride; TQS, 3a,4,5,9b-tetrahydro-4-(1-naphthalenyl)-3*H*-cyclopentan[*c*]quinoline-8-sulfonamide

Molecular Pharmacology Fast Forward. Published on July 24, 2012 as DOI: 10.1124/mol.112.080317
This article has not been copyedited and formatted. The final version may differ from this version.

Abstract

The α7 nicotinic acetylcholine receptors (nAChR) have been a puzzle since their discovery in brain and non-neuronal tissues. Maximal transient P-open of α7 nAChR with rapid agonist applications is only 0.002. The concentration dependence of α7 responses measured from transfected cells and Xenopus oocytes show the same disparity in potency estimations for peak currents and net charge, despite being studied at 1000-fold different time scales. In both cases the EC_{50} was approximately 10-fold lower for net charge than for peak currents. The equivalence of the data obtained at such disparate time scales indicates that desensitization of α7 is nearly instantaneous. At high levels of agonist occupancy, the receptor is preferentially converted to a ligand-bound non-conducting state which can be destabilized by the positive allosteric modulator PNU-120596. Such currents can be sufficiently large to be cytotoxic to the α7-expressing cells. Both the potentiating effect of PNU-120596 and the associated cytotoxicity have a high temperature dependence that can be compensated for by serum factors. Therefore, despite reduced potentiation at body temperatures, use of type II positive allosteric modulators may put cells that naturally express high levels of α7 nAChR, such as neurons in the hippocampus and hypothalamus, at risk. With a low intrinsic open probability and high propensity toward the induction of non-conducting ligand-bound states, it is likely that the well-documented regulation of signal transduction pathways by α7 nAChR in cells such as those that regulate inflammation may be independent of ion channel activation and associated with the non-conducting conformational states.

Molecular Pharmacology Fast Forward. Published on July 24, 2012 as DOI: 10.1124/mol.112.080317
This article has not been copyedited and formatted. The final version may differ from this version.

Introduction

Nicotinic α7 receptors have become one of the most interesting and promising new therapeutic targets since they were first discovered to be the sites of α–bungarotoxin (α-btx) binding in the brain approximately twenty years ago. Data suggest that activation of α7 nicotinic acetylcholine receptors (nAChR), a subtype with uniquely high calcium permeability, can provide cytoprotection, enhance performance in behavioral tasks related to cognitive function, reduce auditory gating deficits seen in schizophrenia (reviewed in (Haydar and Dunlop, 2010; Thomsen et al., 2010)), and modulate inflammation (de Jonge and Ulloa, 2007). Although structurally related to the high affinity nicotine binding sites in the brain and the α-btx-sensitive nAChR of the neuromuscular junction, α7 receptors are in many ways unique from other ligand-gated ion channels and confound our conventional approaches and usual assumptions. In several ways, the α7 nAChR represents a primordial type of receptor. They are functional without being co-assembled with specialized accessory subunits required by other nAChR subtypes (Drisdel and Green, 2000). They are activatible by the ubiquitous acetylcholine (ACh) precursor, choline (Papke et al., 1996), and are found in many types of non-excitable, non-neuronal cells (de Jonge and Ulloa, 2007). They open rather inefficiently, and, although they rapidly desensitize in the presence of high concentrations of agonist, once desensitized they do not convert to a high affinity state, as do other nAChR (Williams et al., 2011c). These are the features that one might imagine would be present in an ion channel of an organism lacking an evolved nervous system with rapid chemical synaptic transmission. They make α7 nAChR invisible to agonist binding experiments, and for many years they were almost impossible to characterize electrophysiologically.

Both academic and industrial labs have discovered numerous agonists with selectivity for α7 (Horenstein et al., 2008), and in recent years an alternative therapeutic approach based on allosteric modulation has gained momentum due to the discovery of many structurally diverse positive allosteric modulators (PAMs) that are selective for α7 receptors (Williams et al., 2011c). To date, the α7 PAMs are classified into one of two categories based on their properties of modulation. The type I PAMs increase the magnitude of α7-mediated responses without large effects on response kinetics. The type II PAMs not only increase the magnitude of responses, but also greatly slow or reverse the decay of macroscopic currents, resulting in very prolonged responses and enormous increases in net charge, which could translate into large changes in intracellular calcium. In addition, the type II PAMs can evoke currents from receptors desensitized by previous agonist applications (Gronlien et al., 2007).

Molecular Pharmacology Fast Forward. Published on July 24, 2012 as DOI: 10.1124/mol.112.080317
This article has not been copyedited and formatted. The final version may differ from this version.

In cases where activation of the α7 ion channel is necessary for a desired therapeutic effect (Briggs et al., 2009), a PAM-based therapeutic approach might offer several potential advantages over agonist-based strategies. However, a PAM-based strategy may also be subject to some potentially important limitations, especially if the potentiation of the calcium-permeable α7 receptor currents becomes so large that calcium homeostasis is disrupted, causing cell death (Lukas et al., 2001; Orr-Urtreger et al., 2000). Nonetheless, *in vivo* studies with α7 PAMs have reported no major concerns regarding toxicity (Williams et al., 2011c), which might suggest that specific factors may prevent over-activation of α7 receptors in the physiological context. We have previously reported that with strong stimulation by the very efficacious PAM *N*-(5-2,4-dimethoxyphenyl)-*N*'-(5-methyl-3-isoxazolyl)-urea (PNU-120596), the majority of the receptors revert to a PAM-insensitive desensitized state (D_i) (Williams et al., 2011b). Additionally, it has been reported that the ability of α7 PAMs to potentiate α7 currents may be significantly reduced at physiological temperature (Sitzia et al., 2011), a factor which would reduce both potential toxicity and therapeutic utility.

To improve our understanding of the unique properties of α7 nAChR, and potential complications that may rise from the use of ostensibly strong PAMs such as PNU-120596, we developed a HEK 293 cell line stably expressing both the human α7 nAChR and the chaperone protein RIC-3 (Treinin, 2008) (A7R3HC10). These cells were used for whole-cell patch-clamp studies which validate previously published models of α7 activation and desensitization that were based on data from the *Xenopus* oocyte expression system. We also characterize the degree to which effects of type I and type II α7 PAMs may be temperature dependent. While temperature can impact the *in vitro* cytotoxicity profile of an α7 PAM, *in vivo* factors may compensate for the effect of temperature.

Molecular Pharmacology Fast Forward. Published on July 24, 2012 as DOI: 10.1124/mol.112.080317
This article has not been copyedited and formatted. The final version may differ from this version.

Materials and Methods

cDNA clones used for stable expression of human alpha7 and human RIC-3 in HEK 293 cells

The human α7 receptor clone was obtained from Dr. Jon Lindstrom (University of Pennsylvania, Philadelphia PA). The human RIC-3 clone was obtained from Dr. Millet Treinin (Hebrew University, Jerusalem Israel) and was co-transfected with α7 to improve receptor expression (Halevi et al., 2002).

Chemicals

Solvents and reagents were purchased from Sigma-Aldrich Chemical Company (St. Louis, MO). The BSA (Fraction V) was from Fisher Scientific (Waltham, MA). PNU-120596 was synthesized by Dr. Jingyi Wang as described in (Williams et al., 2011b). Unlabeled α-btx was purchased from Biotoxins, Inc. (Saint Cloud, FL). [^{125}I] α-btx was prepared and generously provided by Dr. Ralph Loring (Northeastern University, Boston, MA). Cell culture supplies were purchased from Life Technologies (Grand Island, NY). The Hank's balanced saline solution (HBSS) (Life Technologies, Grand Island, NY) contained (in mM): $CaCl_2$ (1.26), $MgCl_2$ (0.493), $MgSO_4$ (0.407), KCl (5.33), KH_2PO_4 (0.441), $NaHCO_3$ (4.17), NaCl (137.93), Na_2HPO_4 (0.338), D-Glucose (5.56). Fresh acetylcholine (ACh) stock solutions were made each day of experimentation. PNU-120596 stock solutions were prepared in DMSO, stored at -20º C, and used for up to 30 days. PNU-120596 solutions were prepared fresh each day at the desired concentration from the stored stock. 5-hydroxyindole (5HI) was purchased from Sigma. NS-1738 was purchased from Tocris (c/o R&D Systems, Minneapolis MN). TQS was generously supplied by Institut De Recherches Internationales Servier (Cedex, France).

Equilibrium radioligand binding assay

Two to three days prior to binding assays, cells were plated in poly-D-lysine-treated 24-well dishes. Experiments were performed when the cells were ~60-80% confluent. The growth media was removed and cells were washed one time with Dulbecco's phosphate buffered saline (Life Technologies, Grand Island, NY). [^{125}I] α-btx containing-solutions (0.05 nM-7 nM) were added to the cells and incubated at room temperature for 3 hours. Non-specific binding was determined with the addition of 1 μM unlabeled α-btx in separate wells. After the 3-hour incubation, the radioligand was removed and the cells were washed three times with cold Dulbecco's phosphate-buffered saline. The cells were then solubilized with 0.1 M NaOH/0.1% SDS and samples were counted in a gamma counter (Beckman Coulter, Brea, CA). Saturation binding curves

Molecular Pharmacology Fast Forward. Published on July 24, 2012 as DOI: 10.1124/mol.112.080317
This article has not been copyedited and formatted. The final version may differ from this version.

were fit to the equation B_{max}[ligand]/(EC_{50} + [ligand]) with Kaleidagraph 3.0.2 (Abelbeck Software; Reading, PA). Each condition was tested in triplicate for each experiment, and each experiment was repeated three independent times.

Cytotoxicity Experiments

The cells were maintained in normal growth medium, and experiments were completed in HBSS. One day prior to performing the toxicity studies, two sets of A7R3HC10 cells from the same passage and two sets of untransfected HEK 293 cells from the same passage were plated in 96-well plates at a density of 15,000 cells per well in normal growth medium (Dulbecco's modified eagle medium (DMEM) with 10% fetal bovine serum (FBS) and incubated at 37 °C with 5% CO_2. Experimental solutions containing the desired concentrations and chemicals of sufficient volume to treat both sets of untransfected HEK 293 cells and both sets of A7R3HC10 cells were prepared in HBSS and then applied to the cells after removing the normal growth medium. One set of A7R3HC10 cells and one set of untransfected HEK 293 cells were placed in an incubator set to 28°C with 5% CO_2. The other set of A7R3HC10 cells and untransfected HEK 293 cells were placed in an incubator set to 37 °C with 5% CO_2. Incubations with experimental treatments were 2 hours since maximal toxicity occurred within 2 hours, as determined from separate experiments evaluating the onset of toxicity at various time points during 24 hours following treatments (data not shown). Following the 2 hour treatment period, the experimental solutions were replaced with 100 μL HBSS and 20 μL per well of CellTiter96 solution (Promega, Madison, WI) and incubated for 2-4 hours at 37 °C with 5% CO_2 after which absorbance readings were made with a microplate spectrophotometer at 490 nm (BioTek, Winooski, VT). Each condition in an experiment was tested in triplicate. The triplicate values were averaged to obtain a mean value for each treatment condition in an individual experiment, and experiments were repeated on at least three independent occasions. Background absorbance was measured from cell-free wells and subtracted from all control and experimental test conditions. Absorbance readings from experimental test conditions were normalized to the absorbance values of untreated/DMSO-vehicle controls, which were defined as 100% cell viability. The DMSO was used to dissolve PNU-120596, which is insoluble in water. The highest concentration of DMSO applied with PNU-120596 was limited to 0.3%, and this occurred in the 30 μM PNU-120596 condition. The 20% DMSO and 30 μM thapsigargin conditions were used as positive controls for toxicity. The statistical significance of PNU-120596 treatments was assessed by comparing the viability values obtained with a given concentration of choline with or without PNU-120596 via two-tailed Student's t-

Molecular Pharmacology Fast Forward. Published on July 24, 2012 as DOI: 10.1124/mol.112.080317
This article has not been copyedited and formatted. The final version may differ from this version.

tests. The comparison was made between choline versus choline and PNU-120596 co-treatment groups, rather than between untreated controls versus choline and PNU-120596 co-treatments, since addition of choline alone tended to increase the apparent cell viabilities relative to the untreated/vehicle controls. Cells with fewer than 30 passages after stable transfection were used in all toxicity experiments.

Whole-cell patch-clamp electrophysiology

Whole-cell responses were recorded using an Axopatch 200 amplifier (Molecular Devices, Union City, CA). In the experiments that involved temperature adjustments, the temperature was controlled with a TC-324B temperature controller (Warner Instruments, Hamden, CT). Cells were bathed in an external solution containing (in mM): NaCl (165), KCl (5), CaCl2 (2), glucose (10), HEPES (5), atropine (0.001), with the pH adjusted to 7.3 with NaOH. Patch pipettes (Sutter Instruments, Novato, CA) were pulled to a tip diameter of ~2 μm, fire-polished to approximately 5 MΩ, and filled with an internal solution containing (in mM): CsCl (147), $MgCl_2$ (2), $CaCl_2$ (1), EGTA (10), HEPES (10), Mg-ATP (5), pH adjusted to 7.3 with CsOH. Cells were held at -70 mV. Recordings were low-pass filtered to 5 kHz and digitized at 50 kHz with a DigiData 1440 or 20 kHz with a DigiData 1322A (Molecular Devices, Union City, CA) using Clampex data acquisition software (Molecular Devices, Union City, CA). A 10 ms test pulse of -10 mV was used to determine access and input resistances prior to each response. For experiments performed at room temperature, whole-cell recordings were analyzed if access resistances were <40 MΩ and membrane resistances were >200 MΩ. On average, the access resistance, membrane resistance, and cell capacitance values were 15.8 ± 0.6 MΩ, 1.55 ± 0.15 GΩ, and 55.2 ± 6.6 pF, respectively. For experiments evaluating the temperature-dependence of PNU-120596, these basic criteria were necessarily relaxed at 37 °C. Sweeps with access resistance <40 MΩ, input resistance >100 MΩ, holding current <700 pA were included in the analysis. No attempt was made to compensate for series resistance or for the liquid junction potential, although the liquid junction potential was calculated to be 4.7 mV. The whole-cell recordings were analyzed with Clampfit 10 (Molecular Devices, Union City, CA).

For the ACh concentration-response and methyllycaconitine (MLA) inhibition curves, rapid drug application to whole-cells was performed with a Burleigh piezoelectric stepper (EXFO, Ontario, Canada) as described previously (Williams et al., 2011a). Theta glass (Sutter Instruments, Novato, CA) was pulled, scored, and then broken by hand to create a drug application pipette with a diameter of 350 μM, which was mounted to the stepper. The voltage signal used to control the piezoelectric stepper was conditioned by

Molecular Pharmacology Fast Forward. Published on July 24, 2012 as DOI: 10.1124/mol.112.080317
This article has not been copyedited and formatted. The final version may differ from this version.

an RC circuit (τ = 2 ms) to reduce oscillations and avoid damage to the crystal. Solution exchange times were 2.6 ± 0.8 ms as determined by measuring holding current shifts (10-90% rise-times) upon moving diluted external solution over an open recording pipette each day of experimentation. The open recording pipette was positioned just above the surface of the recording chamber and in the same arrangement relative to the drug application pipette during a whole-cell recording. It should be stated that the exchange time estimate measured in this manner is probably only a lower-limit (i.e. fastest time possible) of the solution exchange time achieved for a whole-cell during a recording. Three applications of 300 μM ACh were applied initially followed by 3 test applications of 1 μM - 3 mM ACh. Interstimulus intervals were 60 seconds. The responses from the initial 3 responses to 300 μM ACh were averaged, as were the 3 responses from the test concentrations of ACh. The averaged response of each cell to the test ACh concentration was normalized to the averaged response to 300 μM ACh in order to compensate for varying levels of receptor expression among individual cells. The normalized responses were subsequently adjusted to reflect the response relative to the maximal normalized ACh-evoked response, which was defined as 1. Both peak current and net charge responses were measured; net charge responses were measured as the area under the activation curve during one second of ACh application. Means and standard errors were calculated from the responses of 4-8 cells at each test concentration. Experiments for the MLA inhibition curve were performed in a similar manner as the ACh concentration-response curve, with the initial concentration of ACh being 170 μM and test concentrations consisting of 170 μM co-application with 3 nM - 100 μM MLA. No pre-applications of MLA were made. Each data point represents the mean and standard error of 4-6 cells at each test concentration. For concentration-response relationships, the data were plotted using Kaleidagraph 3.0.2 (Abelbeck Software; Reading, PA), and curves were generated as the best fit of the average values to the Hill equation, Response = $(I_{max}[agonist]^n)/([agonist]^n + (EC_{50})^n)$, where I_{max} denotes the maximal normalized response and n represents the Hill coefficient. I_{max} values of the curve fits were constrained to equal 1. In the case of the MLA inhibition concentration-response relationship, negative Hill slopes were used. Error estimates of the EC_{50} values are the standard errors of the parameters based on the Levenberg-Marquardt algorithm used for the generation of the fits (Press, 1988).

In all other whole-cell electrophysiology experiments, local applications of drug were made using single-barrel glass pipettes attached to a picospritzer (General Valve, Fairfield, NJ) with Teflon tubing (11.5-14.5 psi). The application pipette was placed within 10-15 μm of the cell. Drug applications were 3 seconds in duration and were

made every 60 seconds. Drugs applied with this method were determined to be diluted 1.5-fold by the time they reached the cell surface (see Supplemental Data). In the temperature experiments, 3 baseline responses were recorded at room temperature (23.5 °C), after which responses were recorded as the temperature was increased to 37 °C. Three responses were recorded at 37 °C and then the temperature was returned to 23.5 °C. Cells with responses that failed to recover to 50% of the average baseline response upon temperature reduction from 37 °C to 23.5 °C were excluded from analysis; 6 of 70 total cells failed to meet this criterion. Responses were measured as peak currents. In most cases, the currents recorded at 37 °C were normalized to the average peak amplitude of the three initial baseline responses recorded at 23.5 °C. It is important to note that at 37 ºC the quality of the whole-cell seals usually decreased. Because of this, the parameters used to define an acceptable whole-cell recording at 37 ºC were more relaxed than they would be for a typical whole-cell recording made at room temperature. Whole-cell seals with access resistance <40 MΩ, input resistance >100 MΩ, and holding current <700 pA at 37 °C were included in the analysis. Prior to the increase in temperature, access resistances were <15 MΩ, input resistances were >1 GΩ, and the holding current was between -50 pA and 0 pA. In most cases, if the patch survived the time at 37 ºC, the whole-cell parameters improved as temperatures returned to room temperature.

In comparing the effect of BSA on potentiation by PNU-120596 at 37 °C, responses are shown as both normalized currents and the absolute magnitude of evoked currents. To test for the statistical significance of BSA on PNU-120596 potentiation at 23.5 °C or 37 °C, the sweeps obtained from each cell at 23.5 °C or 37 °C were averaged to obtain one mean response from each cell at 23.5 °C or 37 °C. The mean responses from cells recorded at 23.5 °C or 37 °C either in the absence or presence of 30 μM BSA were then compared with a two-tailed Student's t-test using Microsoft Excel (Microsoft, Redmond, WA).

Molecular Pharmacology Fast Forward. Published on July 24, 2012 as DOI: 10.1124/mol.112.080317
This article has not been copyedited and formatted. The final version may differ from this version.

Results

The concentration dependence of ACh-evoked peak current and net charge responses from A7R3HC10 cells

The ACh concentration-response relationship for ACh-evoked whole-cell currents using a rapid solution switching onto A7R3HC10 cells resulted in non-superimposable curves for peak current and net charge measurements, as expected for α7 receptors (Figure 1). The EC_{50} values determined from peak currents and net charge were 167 ± 20 μM and 26 ± 6 μM, respectively. Note that these values are not significantly different from those previously reported for human α7 nAChRs expressed in *Xenopus* oocytes, 173 ± 8 and 21 ± 3 for peak currents and net charge, respectively (Papke and Papke, 2002) even though the time scale of the responses was a thousand-fold faster than that of oocyte recording.

The curve for net charge was fit between the 1 μM ACh and 300 μM ACh points since the net charge was reduced from the maximum at ACh concentrations above 300 μM. A unique feature of the α7 receptor is the concentration-dependent desensitization that is rapidly induced with applications of high agonist concentrations. The reductions in net charge at high concentrations seen in this experiment were more pronounced than normally occurs in oocyte experiments. This was likely due to differences in the presentation of agonist; drug applications were made here with a system that provided solution exchanges on the order of several milliseconds versus the drug delivery that occurs on a time scale of 3-4 seconds in a typical oocyte experiment. The rapid application of high agonist concentrations produced synchronous activation and desensitization of the α7 receptor population, resulting in extremely sharp macroscopic responses with minimal area (Figure 1A). This is also demonstrated by comparing the rise-times and rise-slopes with increasing concentrations of ACh; the 10-90% rise-times became shorter and the 10-90% rise-slopes became steeper as ACh concentrations increased (Table 1). The peak in the responses to the applications of 1 mM or 3 mM ACh occurred faster than the solution exchange, indicating that the maximal synchronous channel opening occurs at ACh concentrations substantially lower than these high concentrations, which would likely saturate the agonist binding sites. This is consistent with channel activation occurring with highest probability when there is only partial occupancy of the multiple binding sites (Williams et al., 2011a; Williams et al., 2011b).

Calibration of ACh-evoked currents based on specific binding of [125I]-α-Btx to intact A7R3HC10 *Cells*

Molecular Pharmacology Fast Forward. Published on July 24, 2012 as DOI: 10.1124/mol.112.080317
This article has not been copyedited and formatted. The final version may differ from this version.

We wished to obtain an estimate of the total number of receptors contributing to the ACh-evoked responses of A7R3HC10 cells. Specific labeling with 3 nM [^{125}I]-α-btx was observed in intact A7R3HC10 cells, while no specific labeling was detected in untransfected HEK 293 cells treated in parallel with the same solutions (Figure 2A). From three saturation binding experiments to intact cells, the K_d of α-btx was 991 ± 67 pM and the B_{max} was 7.7 x 10^{-8} ± 1.3 x 10^{-8} pmol/cell (Figure 2B-C). This B_{max} translates to an average of 9,300 ± 1,500 receptors expressed/cell assuming that 5 molecules of radiolabeled α-btx were bound to each α7 receptor (Palma et al., 1996).

The average peak current and net charge evoked by 300 μM ACh from A7R3HC10 cells (n = 33) was 163 ± 26 pA and 9,800 ± 1,500 pA*ms, respectively. The single-channel amplitude of α7 channels (potentiated by PNU-120596) was determined to be approximately 7.8 pA (Williams et al., 2011b); this means that ~20 α7 channels were open at the peak of an average current. If an average cell expresses 9,300 α7 ion channels, and all of those ion channels are equally activatible just prior to the agonist stimulation, the probability of an α7 receptor being open (P_{open}) at the peak of the current evoked by 300 μM ACh is approximately 0.002. Assuming an average single-channel open lifetime of 0.1 ms (Williams et al., 2011b), an average net charge response to a one second application of 300 μM ACh contains ~12,000 channel openings. Based on these numbers, individual channels opened on average only 1.3 times during the one second of 300 μM ACh application. These numbers are certainly rough estimates, but they suggest that the instantaneous P_{open} of α7 is never high, not even immediately after the presentation of a strong agonist stimulus, and that an average individual α7 channel opens less than 2 times before becoming desensitized in response to 300 μM ACh. The reduced net charge observed with the application ACh concentrations higher than 300 μM is also indicative of lower P_{open} with higher levels of agonist occupancy. Under steady-state conditions where ACh is presented for prolonged periods of time, the α7 P_{open} will also be substantially less than the estimated maximum of 0.002 due to desensitization. The peak current of PNU-120596-potentiated responses from outside-out patches was previously used to obtain a lower limit of the number of channels in a patch. This lower-limit estimate of channel number was used to estimate that the upper limit of the α7 P_{open} during a 12-second application of 60 μM ACh is 7.4 x 10^{-6} ± 3.0 x 10^{-6} (Williams et al., 2011b).

Evaluation of the in vitro cytotoxicity profile of PNU-120596 in A7R3HC10 cells

We have previously characterized the potentiating activity of PNU-120596 on single α7 receptors in outside-out patches from transiently transfected HEK 293 cells

Molecular Pharmacology Fast Forward. Published on July 24, 2012 as DOI: 10.1124/mol.112.080317
This article has not been copyedited and formatted. The final version may differ from this version.

(Williams et al., 2011b). We confirmed that the α7-mediated whole-cell currents of A7R3HC10 cells were similarly sensitive to this type II PAM (Figure 3). Similar to what we have reported for α7 currents in oocytes, with these responses activated by pressure application of ACh or ACh plus PNU-120596, there was a modest increase in peak current and a 100-fold larger increase in net charge. The potentiated currents increased throughout the pressure application, while, as expected, the current evoked by the relatively high concentration of ACh alone decayed to baseline rapidly while the agonist pulse was still occurring.

Neuronal α7 receptors have a high relative permeability to calcium (Seguela et al., 1993), and the generation of large calcium-rich current such of those promoted by co-applications of PNU-120596 with agonists might be likely to perturb the calcium homeostasis of the α7-expressing cells past the "set point" which most effectively promotes cell survival (Johnson et al., 1992). Contradictory results have been published regarding the *in vitro* cytotoxic effects of PNU-120596 (reviewed in (Williams et al., 2011c)). In contrast to previous studies, which tested limited agonist and/or PAM concentrations, we wished to assess the potential toxicity profile of PNU-120596 over a range of agonist and PNU-120596 concentrations with the A7R3HC10 cell line. Based on the recent finding that high concentrations of agonist and PNU-120596 promote non-conducting D_i states (Williams et al., 2011b), maximal cytotoxicity was hypothesized to occur upon treatment with relatively low concentrations of both agonist and PNU-120596 since this condition produces the greatest degree of ion channel activation over time. In addition, the existence of D_i states were hypothesized to account for the discrepancy in the literature regarding the toxicity of PNU-120596, given that the two studies (Dinklo et al., 2011; Ng et al., 2007) reporting PNU-120596 toxicity used 100 μM choline as the agonist, while the one study (Hu et al., 2009) that reported a lack of PNU-120596 toxicity used a very strong agonist stimulus that potentially stabilized D_i states.

Note that in these experiments we chose to use choline, rather than ACh, as the stimulating agonist to avoid issues that may accompany the labile nature of ACh. Choline has been shown to selectively activate α7 nAChRs with similar efficacy to ACh, although with approximately 10-fold lower potency (Papke et al., 1996). We based our measurements of "cytotoxicity" or "reductions in cell viability" on the reduction of a tetrazolium salt (CellTiter96 Reagent; Promega, Madison, WI) by dehydrogenase enzymes in metabolically active cells to a soluble formazan dye, the quantity of which is directly related to absorbance at 490 nm.

Initial cytotoxicity experiments were performed in full rich DMEM media containing 10% FBS with treatments incubated at 37 ºC. A range of choline

Molecular Pharmacology Fast Forward. Published on July 24, 2012 as DOI: 10.1124/mol.112.080317
This article has not been copyedited and formatted. The final version may differ from this version.

concentrations between 0 and 3 mM were co-applied with 10 μM PNU-120596, and in these experiments cell viabilities were reduced to approximately 15-25% of the controls whenever PNU-120596 was applied (data not shown), even without additional choline. Since PNU-120596 applied alone without agonist caused the same degree of toxicity as when applied with agonist, we conducted all further experiments under more defined conditions which would allow us to better determine whether cytotoxic effects on PNU-120596 were indeed dependent on α7 receptor activation.

When experiments were performed in HBSS, treatments with PNU-120596 alone failed to produce cytotoxicity, and all future experiments were performed in HBSS. However, when choline was co-applied with PNU-120596 and cells were incubated at 37 °C in HBSS, there was likewise no significant degree of toxicity was observed for any of the choline and PNU-120596 combinations (Figure 4).

Temperature-dependence of PNU-120596 on potentiation of α7-mediated responses.

It has recently been reported that the potentiation of responses by the α7 PAMs PNU-120596 and SB-206553 may have a dependence on the temperature, with potentiation being drastically reduced near physiological temperatures (Sitzia et al., 2011). To investigate the effect of temperature on α7 PAM efficacy, we tested the activities of type I and type II PAMs at 37 ºC with whole-cell recordings from the A7R3HC10 cell line. Control experiments (Supplemental Figure 5) were conducted to determine the response stability at a fixed temperature and determine the effects of temperature on responses to ACh alone. In rundown control experiments performed without temperature adjustments, the amplitude of the responses at the end of the experiment were ~70% of the responses at the beginning.

To determine the temperature effects on the α7-mediated currents, we obtained three responses at room temperature (23.5 °C), progressively increased the temperature, recorded three responses at 37 °C, and then reduced the temperature back down to 23.5 °C. When 1 mM ACh was applied alone, peak currents at 37 °C were 47 ± 3% of the initial baseline currents recorded at 23.5 °C, and they recovered to ~80% upon temperature reduction back to 23.5 °C, a full recovery relative to the rundown control (Supplemental Figure 5 C-D and Table 2).

When 10 μM PNU-120596 was co-applied with 100 μM ACh, potentiated responses at 37 °C were reduced to a much greater extent relative to 23.5 °C than the response reduction that occurred when 1 mM ACh was applied alone (Figure 5A-B and Table 2). At 37 ºC PNU-120596-potentiated responses were only 12 ± 3% (88% reduction) of the baseline responses obtained initially at 23.5 °C, but recovered when the

Molecular Pharmacology Fast Forward. Published on July 24, 2012 as DOI: 10.1124/mol.112.080317
This article has not been copyedited and formatted. The final version may differ from this version.

temperature was returned to 23.5 °C. This result is consistent with recent findings (Sitzia et al., 2011) and predicts that there may be temperature-dependence of the PNU-120596 cytotoxicity. However, since recent studies of the concentration-dependence of PNU-120596 potentiation (Williams et al., 2011b) suggest that potentiation may be reduced with high concentrations of the agent due to the induction of resistant forms of desensitization, producing an inverted U concentration response relationship, we also wished to test whether temperature might have the effect of shifting this concentration-response relationship so that potentiation by a lower concentration of PNU-120596 might show less temperature sensitivity. We tested this hypothesis by repeating the temperature experiment with a 10-fold lower concentration of PNU-120596. The result with 1 μM PNU-120596 was similar to that with 10 μM PNU-120596 (Figure 5C-D and Table 2). When 1 μM PNU-120596 was co-applied with 100 μM ACh, potentiated responses at 37 °C were 13 ± 3% (87% reduction) of the initial responses at 23.5 °C, and then recovered when the temperature was returned to room temperature.

To determine if the apparent temperature sensitivity of PNU-120596 is applicable to other PAMs, the protocol was repeated with the type I PAMs 5-HI and NS-1738 and the alternative type II PAM TQS (Gronlien et al., 2007) (Supplemental Figure 6). The effects of temperature on potentiation of responses evoked by 100 μM ACh with either 1 mM 5-HI or 10 μM NS-1738 were similar (Table 2). Relative to baseline responses at room temperature, at 37 ˚C 1 mM 5HI-potentiated responses were 33 ± 2% (67% reduction), and 10 μM NS-1738 potentiated responses were 34 ± 5% (66% reduction). Neither of these effects were significantly larger than the reduction seen with ACh alone ($p<0.05$). In both cases the potentiated responses recovered when temperatures returned to 23.5 °C to an extent expected (~70-80%) based on the rundown control.

Likewise, the potentiation of 100 μM ACh-evoked responses by 10 μM TQS was not reduced any more at 37 °C than the reduction in response amplitude that occurred when ACh was applied alone (Supplemental Figure 6 and Table 2). At 37 °C the responses potentiated by TQS were 46 ± 3% (54% reduction) of the baseline responses and recovered to the level of the rundown controls when the temperature was returned to 23.5 ˚C.

Effect of temperature on PNU-120596 cytotoxicity

Our data indicate that amongst the agents tested, temperature had a uniquely large effect on potentiation by PNU-120596. Therefore we re-evaluated the PNU-120596 for potential toxic effects at 28°C. Significant toxicity was observed when treatments were incubated at 28°C in HBSS in a manner that was dependent on the concentration of PNU-

Molecular Pharmacology Fast Forward. Published on July 24, 2012 as DOI: 10.1124/mol.112.080317
This article has not been copyedited and formatted. The final version may differ from this version.

120596 and, to a lesser extent, on the concentration of choline (Figure 6). Applications of choline alone or PNU-120596 alone did not reduce cell viabilities, although choline had a tendency to increase the viability relative to the control cells. No significant toxicity was produced with 1 μM PNU-120596 over the range of choline concentrations tested; however, at 3 μM PNU-120596 statistically significant toxicity was observed with 1 mM and 3 mM choline co-applications. The greatest degree of toxicity was observed when choline was applied with 10 μM PNU-120596, for all concentrations of choline tested, resulting in approximately 50% cell viabilities relative to the controls. Interestingly, consistent with an inverted U concentration response, with 30 μM PNU-120596, significant reductions in cell viability were only observed when co-applications were made with 100 μM and 1 mM choline, and the magnitude of toxicity in this case was less than what was observed when treatments included 10 μM PNU-120596. None of the choline and/or PNU-120596 treatments had toxic effects on untransfected HEK293 cells (data not shown).

Cytotoxic effects of PNU-120596 are MLA-sensitive

To confirm that the observed toxicity occurred via α7 nAChRs, the competitive antagonist MLA was given at varying time points relative to toxic 100 μM choline and 10 μM PNU-120596 co-treatments incubated at 28°C. As shown in Figure 7, neither a 10 minute pre-application nor co-application of 10 nM MLA was able to block the toxicity produced by the choline and PNU-120596 co-application. However, this is consistent with the recent observation that 10 nM applications of MLA on top of steady-state currents elicited by choline and PNU-120596 actually transiently increase current rather than inhibit current, suggesting that low concentrations of MLA may alter the equilibrium between D_s and D_i towards D_s (Williams et al., 2011b). Application of a 10-fold higher MLA concentration either 10 minutes before or with 100 μM choline and 10 μM PNU-120596 co-treatment was able to completely block the toxic effect, confirming that the toxicity is mediated by α7 receptors. In contrast, 100 nM MLA was unable to block the effect if it was applied 10 minutes after the toxic 100 μM choline and 10 μM PNU-120596 co-treatment. This suggests that the onset of PNU-120596-induced toxicity in these cells occurs rapidly, in less than 10 minutes.

Bovine serum albumin modulation of PNU-120596 toxicity and potentiation activity

As stated above, we noted that in preliminary experiments treatments with 10 μM PNU-120596 alone were toxic at 37 ºC when the solutions were prepared in DMEM with 10% FBS. Since both the media and FBS are choline-containing, it is not too surprising

Molecular Pharmacology Fast Forward. Published on July 24, 2012 as DOI: 10.1124/mol.112.080317
This article has not been copyedited and formatted. The final version may differ from this version.

that the PNU-120596 effects did not require added agonist; however, it was unclear why the activity was present at 37 ˚C, given the effects of temperature on PNU-120596 potentiation and toxicity in HBSS. We therefore tested the hypothesis that the FBS supplied a factor that augmented the potentiating effects of PNU-120596, or reversed the temperature sensitivity of PNU-120596 potentiation.

Solutions were therefore prepared with choline and 10 μM PNU-120596 in HBSS supplemented with 10% FBS. As seen in Figure 8A-B, the presence of FBS eliminated the temperature-dependence of the PNU-120596 toxicity. Bovine serum albumin is a primary constituent of FBS and select serum albumins were previously shown to potentiate α7 nAChR-mediated responses (Conroy et al., 2003). Therefore, the experiments were repeated in HBSS solutions containing 30 μM BSA, the approximate concentration of BSA found in solutions containing 10% FBS (Giles and Czuprynski, 2003; Granato et al., 2003). Again, the temperature-dependence of cytotoxicity induced by PNU-120596 was eliminated (Figure 8C-D), suggesting that BSA is the constituent of FBS primarily responsible for the effect. Given that BSA is a non-specific carrier of hormones and fatty acids in blood plasma, it is possible that a substance bound to the BSA is responsible for the effect, rather than BSA itself. Nonetheless, this observation suggests that although the ability of PNU-120596 to potentiate α7-mediated current at physiological temperature is reduced, some factors are likely to exist *in vivo* that maintain the activity to PNU-120596 at physiological temperatures.

To confirm that the PNU-120596 toxic effects in the BSA-containing HBSS were α7-receptor activation dependent, we tested for sensitivity to the α7-selective competitive antagonist MLA. Additionally, to determine if it required α7 ion channel currents, we also tested the non-competitive antagonist mecamylamine (Figure 9). As before, 10 nM MLA was unable to completely block the toxic effect of the treatment. Ten minute pre-applications and co-applications of 100 nM MLA completely reversed the toxicity, while applications of MLA 10 minutes or more after the choline and PNU-120596 treatment had no apparent effect. In addition, 10-minute pre-treatment and co-treatment with 100 μM mecamylamine was able to partially block the toxicity of choline and PNU-120596 treatment, while mecamylamine treatments 10 minutes or more after the treatment had no effect. The IC_{50} for mecamylamine on α7 nAChR was approximately 10 μM in experiments performed in oocytes where mecamylamine was co-applied with 300 μM ACh (Papke et al., 2001). In addition, 100 μM mecamylamine appears to fully block steady-state currents generated by choline and PNU-120596 co-application in recent experiments (Williams et al., 2011b). Although the 100 μM concentration of mecamylamine was unable to completely block the toxic effect in these studies, the

Molecular Pharmacology Fast Forward. Published on July 24, 2012 as DOI: 10.1124/mol.112.080317
This article has not been copyedited and formatted. The final version may differ from this version.

partial block that was observed combined with the rapid onset of the toxicity in less than 10 minutes is consistent with a requirement for direct ion channel activity.

Effects of BSA on the temperature-dependence of PNU-120596 potentiation.

Since 30 μM BSA appeared to eliminate the temperature-dependence of PNU-120596 cytotoxicity in a manner that was dependent on α7 nAChR signaling, whole-cell electrophysiology experiments were performed in the presence of 30 μM BSA. When the responses recorded with 30 μM BSA at 37 °C were expressed relative to the initial responses obtained at 23.5 °C, the effect of BSA on the normalized peak currents was not statistically significant (Figure 10A and Table 2; $p > 0.05$). However, when the same data were plotted based on the absolute magnitude of the recorded peak currents, the responses recorded in the presence of 30 μM BSA at 23.5 °C and 37 °C were significantly larger than responses recorded in the absence of BSA (Figure 10B; $p < 0.05$). On average, the peak currents evoked by 100 μM ACh and 10 μM PNU-120596 co-application at 23.5 °C in the absence and presence of 30 μM BSA were 1,300 ± 400 pA and 2,800 ± 300 pA, respectively. The average peak currents recorded at 37 °C in the absence and presence of 30 μM BSA were 100 ± 30 pA and 390 ± 100 pA, respectively. Our data suggest that 30 μM BSA potentiates α7-mediated responses in an additive manner with PNU-120596 that is not temperature sensitive.

Molecular Pharmacology Fast Forward. Published on July 24, 2012 as DOI: 10.1124/mol.112.080317
This article has not been copyedited and formatted. The final version may differ from this version.

Discussion

Our studies of the α7-mediated currents evoked by rapid ACh applications provide valuable insights into the unique activation and desensitization properties of this receptor and allow us to provide, for the first time, an estimate of the maximal non-stationary P_{open} of this receptor. Our estimate of 0.002 is in remarkable contrast to the values of 0.7 to 0.8 for heteromeric receptors such as α4β2 (Li and Steinbach, 2010) and muscle-type receptors (Land et al., 1981).

The decrease in net charge in the responses evoked during concentration ramps that approached final ACh concentrations over 300 μM is consistent with the hypothesis that the transient α7 peak P_{open} is further reduced at high levels of agonist occupancy, supporting a model we have previously proposed (Papke et al., 2000a; Williams et al., 2011b) based in part on oocyte experiments. However, conclusions based on slow macroscopic responses may sometimes be questionable. For example, the peak currents of heteromeric receptor macroscopic oocyte currents are more likely to represent a condition incorporating a large degree of steady-state desensitization than conditions of maximal P_{open} (Papke, 2009). However, this is not the case with the α7 responses, which appear to reflect instantaneous agonist concentration (Papke and Thinschmidt, 1998), regardless of how slowly or rapidly agonist concentration changes (Papke et al., 2000b; Uteshev et al., 2002). The data from the present study, obtained on a millisecond time scale, showed concentration-response relationships for peak current and net charge that were essentially identical to those reported for the oocyte responses, despite a thousand-fold difference in the time scales of the recordings. This supports the hypothesis that the kinetics of the responses in both systems are following the instantaneous changes in agonist concentration and, by inference, the levels in agonist occupancy. The primary difference between the A7R3HC10 ACh concentration-response data and those from oocytes (Papke and Papke, 2002) was that, with the very rapid high concentration ramps applied to the cells, receptors were not at the optimal range of agonist occupancy long enough for maximal net charge responses to occur.

The therapeutic utility of PAMs for ligand-gated ion channels of the Cys-loop receptor family has been amply proven by the development of benzodiazepines, $GABA_a$ receptor PAMs. Benzodiazepines were preceded in clinical development by barbiturates, which have a larger spectrum of effects than benzodiazepines and subsequently a significantly smaller therapeutic index. With the recognition of α7 as a potentially important therapeutic target, α7 PAMs also appear to be an attractive approach for new drug development. Just as benzodiazepines can be distinguished from barbiturates, we

Molecular Pharmacology Fast Forward. Published on July 24, 2012 as DOI: 10.1124/mol.112.080317
This article has not been copyedited and formatted. The final version may differ from this version.

can distinguish type I and type II α7 PAMs, with the type II agents appearing to have such high efficacy that they might lead to unregulated activation.

With a type II PAM the tonic presence of the α7 agonist choline could disrupt native signaling dynamics and, if the potentiation of the calcium permeable receptor currents becomes sufficiently large to disrupt calcium homeostasis, cause cell death (Lukas et al., 2001; Orr-Urtreger et al., 2000). This could be especially true in cases of trauma or stroke, when choline concentrations in the brain increase to as high as 100 μM (Jope and Gu, 1991; Scremin and Jenden, 1991).

Of the PAMs tested, only PNU-120596 showed strong temperature-dependent potentiation. This is despite the fact that TQS is also a type II PAM, and that PNU-120596 and NS 1738 share the common structural feature of a central urea group. The data suggest that, although PNU-120596 and TQS have similar potentiating properties, they work through distinct mechanisms. Although PNU-120596 and TQS appear to bind at similar sites in the intrasubunit cavity formed by the four membrane-spanning helices (Gill et al., 2011; Young et al., 2008), there may be alternate protein/PAM interactions, with increased differences in the response to membrane fluidity changes that occur at higher temperature. Although increased temperature had only a modest effect on receptor activation by the allosteric agonist 4BP-TQS (Jindrichova et al., 2012), Sitzia *et al*., 2011 reported that the potentiating activity of SB-206553, a PAM with properties intermediate to the type I and type II PAM classes (Dunlop et al., 2009)) was also reduced at 37°C. While the published data agree that type I PAMs appear to lack *in vitro* cytotoxicity (at the concentrations of agonists and modulators tested), the data are contradictory regarding the *in vitro* toxicity of the type II PAM PNU-120596 (Dinklo et al., 2011; Hu et al., 2009; Ng et al., 2007). *In vivo* studies with α7 PAMs have reported no major concerns regarding toxicity, which might suggest that specific factors can prevent over-activation of α7 receptors in a physiological context. Even for the temperature-sensitive agent PNU-120596, endogenous potentiating factors may provide for a narrow margin of safety for cells expressing high levels of α7 receptors, although it should be noted that the peak current of the A7R3HC10 cells are approximately two-to-three-fold higher than what we have previously reported for α7-expressing cells in hippocampal (Lopez-Hernandez et al., 2007) or hypothalamic brain slices (Uteshev et al., 2003).

A major concern for considering PAM-based therapeutics is whether a PAM will allow α7 receptors to perform their usual functions more effectively or whether they will force α7 receptors into playing alternative roles. To approach the answer to that question, the first step must be to consider exactly what the usual functions of α7 may be,

Molecular Pharmacology Fast Forward. Published on July 24, 2012 as DOI: 10.1124/mol.112.080317
This article has not been copyedited and formatted. The final version may differ from this version.

and how effectively those functions will be amplified by PAMs that work through altering the P_{open} of the receptor's ion channel. As we confirm in these experiments, α7 receptor ion channels are intrinsically rather inefficient compared to other nAChR. This has led to the proposal that α7 receptors are most effective at integrating low-level signals over long periods of time. They desensitize rapidly, but also resensitize rapidly (Mansvelder and McGehee, 2000; Wooltorton et al., 2003). Low concentrations of the α7-selective partial agonist 3-(2,4-dimethoxybenzylidene)anabaseine (GTS-21) can promote the survival of NGF-differentiated PC12 cells after trophic factor withdrawal, provided that the cells are maintained in GTS-21 for several hours. In contrast, treatment of PC12 cells with a high concentration of GTS-21, sufficient to produce a large synchronous current followed by profound desensitization, was toxic to the cells, and the toxic effect was nearly instantaneous (Li et al., 1999). These two treatment paradigms had different effects on intracellular signaling pathways, highlighting a potential dichotomy in functional roles for α7 receptors.

Our understanding of α7 receptors has arguably been encumbered by the usual assumption that α7 function relies entirely on ion channel activation. Nonetheless, α7 receptors have been shown to modulate numerous intracellular signal transduction pathways, in many cases under conditions where it has not been possible to demonstrate a requirement for ion channel activation (Arredondo et al., 2006; de Jonge et al., 2005) (Marrero and Bencherif, 2009; Parrish et al., 2008). In many cases, although clearly dependent on the presence of α7 and stimulation of α7 by putative agonists, the activation of the signal transduction mechanisms appear to be independent of α7 ion channel activation (de Jonge and Ulloa, 2007; Suzuki et al., 2006). These observations support the hypotheses that α7 receptors may function in multiple ways and that various ligands differ in their ability to stimulate ion channel activation and/or signal transduction. Ligands like GTS-21 and NS-6740 (Briggs et al., 2009) that are poor ion channel activators, but are very effective for PNU-120596-induced activation of desensitized receptors (Papke et al., 2009), may also be effective for ion-channel-independent signal transduction. Much of the α7–mediated signal transduction data has come from studies of α7–mediated suppression of inflammation, and the low efficacy, strongly desensitizing agent GTS-21 has been shown to be very effective in several of these models (Giebelen et al., 2007a; Giebelen et al., 2007b; Kageyama-Yahara et al., 2008; Pavlov et al., 2007; van Westerloo et al., 2006). This would suggest that there may be one or more ligand-bound states in which the ion channel activation mechanism is "desensitized" but the receptor otherwise activated, generating a ligand-bound non-

Molecular Pharmacology Fast Forward. Published on July 24, 2012 as DOI: 10.1124/mol.112.080317
This article has not been copyedited and formatted. The final version may differ from this version.

conducting activated state. These may include the state(s) that the type II PAMs convert into conducting states.

If α7 receptors are capable of both channel-mediated and channel-independent signaling, then it may be that PAMs will augment one type of function but not the other. Although our data would caution against the therapeutic development of strong type II PAMs, in cases where activation of the α7 ion channel is necessary for a desired therapeutic effect (Briggs et al., 2009), a type I PAM-based therapeutic approach might offer several potential advantages over agonist-based strategies. The temporal firing dynamics of native cholinergic signaling should be conserved since PAMs would theoretically only augment the response provided by endogenous agonists.

Clearly there is still much more to be learned about α7 nAChR. One challenge that now exists is to define experimental models that might be able to discriminate between channel-dependent and channel-independent α7 functions. The α7 PAMs are therapeutic leads which may also serve as probative tools for the study of these two different forms of signaling, as will ligands like GTS-21 and NS-6740 that may selectively activate specific signaling modes.

Molecular Pharmacology Fast Forward. Published on July 24, 2012 as DOI: 10.1124/mol.112.080317
This article has not been copyedited and formatted. The final version may differ from this version.

Acknowledgements

We thank Dr. Ralph Loring (Northeastern University, Boston, MA) for providing the [^{125}I]-α-btx used in the binding assay. We thank Dr. Cecilia Gotti (University of Milan, Italy) for providing α7 antibodies used in the western blot. We thank Dr. Stephen Baker and Debbie Otero for assistance in conducting the binding assays, Monica Santisteban for conducting the immunoprecipitation and western blot, Institut De Recherches Internationales Servier for supplying TQS and NS-1738, and Drs. Jingyi Wang and Nicole Horenstein for supplying PNU-120596 and for many helpful discussions.

Authorship Contributions

Participated in research design: Williams, Peng, and Papke
Conducted experiments: Williams, Peng, and Kimbrell
Performed data analysis: Williams and Peng
Wrote or contributed to the writing of the manuscript: Williams and Papke

Molecular Pharmacology Fast Forward. Published on July 24, 2012 as DOI: 10.1124/mol.112.080317
This article has not been copyedited and formatted. The final version may differ from this version.

References

Arredondo J, Chernyavsky AI, Jolkovsky DL, Pinkerton KE and Grando SA (2006) Receptor-mediated tobacco toxicity: cooperation of the Ras/Raf-1/MEK1/ERK and JAK-2/STAT-3 pathways downstream of alpha7 nicotinic receptor in oral keratinocytes. *FASEB J* **20**(12):2093-2101.

Briggs CA, Gronlien JH, Curzon P, Timmermann DB, Ween H, Thorin-Hagene K, Kerr P, Anderson DJ, Malysz J, Dyhring T, Olsen GM, Peters D, Bunnelle WH and Gopalakrishnan M (2009) Role of channel activation in cognitive enhancement mediated by alpha7 nicotinic acetylcholine receptors. *Br J Pharmacol* **158**(6):1486-1494.

Conroy WG, Liu QS, Nai Q, Margiotta JF and Berg DK (2003) Potentiation of alpha7-containing nicotinic acetylcholine receptors by select albumins. *Mol Pharmacol* **63**(2):419-428.

de Jonge WJ and Ulloa L (2007) The alpha7 nicotinic acetylcholine receptor as a pharmacological target for inflammation. *Br J Pharmacol* **151**(7):915-929.

de Jonge WJ, van der Zanden EP, The FO, Bijlsma MF, van Westerloo DJ, Bennink RJ, Berthoud HR, Uematsu S, Akira S, van den Wijngaard RM and Boeckxstaens GE (2005) Stimulation of the vagus nerve attenuates macrophage activation by activating the Jak2-STAT3 signaling pathway. *Nat Immunol* **6**(8):844-851.

Dinklo T, Shaban H, Thuring JW, Lavreysen H, Stevens KE, Zheng L, Mackie C, Grantham C, Vandenberk I, Meulders G, Peeters L, Verachtert H, De Prins E and Lesage AS (2011) Characterization of 2-[[4-fluoro-3-(trifluoromethyl)phenyl]amino]-4-(4-pyridinyl)-5-thiazoleme thanol (JNJ-1930942), a novel positive allosteric modulator of the {alpha}7 nicotinic acetylcholine receptor. *J Pharmacol Exp Ther* **336**(2):560-574.

Drisdel RC and Green WN (2000) Neuronal alpha-bungarotoxin receptors are alpha7 subunit homomers. *J Neurosci* **20**(1):133-139.

Dunlop J, Lock T, Jow B, Sitzia F, Grauer S, Jow F, Kramer A, Bowlby MR, Randall A, Kowal D, Gilbert A, Comery TA, Larocque J, Soloveva V, Brown J and Roncarati R (2009) Old and new pharmacology: positive allosteric modulation of the alpha7 nicotinic acetylcholine receptor by the 5-hydroxytryptamine(2B/C) receptor antagonist SB-206553 (3,5-dihydro-5-methyl-N-3-pyridinylbenzo[1,2-b:4,5-b']di pyrrole-1(2H)-carboxamide). *J Pharmacol Exp Ther* **328**(3):766-776.

Giebelen IA, van Westerloo DJ, LaRosa GJ, de Vos AF and van der Poll T (2007a) Local stimulation of alpha7 cholinergic receptors inhibits LPS-induced TNF-alpha release in the mouse lung. *Shock* **28**(6):700-703.

Giebelen IA, van Westerloo DJ, LaRosa GJ, de Vos AF and van der Poll T (2007b) Stimulation of alpha 7 cholinergic receptors inhibits lipopolysaccharide-induced neutrophil recruitment by a tumor necrosis factor alpha-independent mechanism. *Shock* **27**(4):443-447.

Giles S and Czuprynski C (2003) Novel role for albumin in innate immunity: serum albumin inhibits the growth of Blastomyces dermatitidis yeast form in vitro. *Infect Immun* **71**(11):6648-6652.

Gill JK, Savolainen M, Young GT, Zwart R, Sher E and Millar NS (2011) Agonist activation of {alpha}7 nicotinic acetylcholine receptors via an allosteric transmembrane site. *Proc Natl Acad Sci U S A* **108**(14):5867-5872.

Granato A, Gores G, Vilei MT, Tolando R, Ferraresso C and Muraca M (2003) Bilirubin inhibits bile acid induced apoptosis in rat hepatocytes. *Gut* **52**(12):1774-1778.

Gronlien JH, Haakerud M, Ween H, Thorin-Hagene K, Briggs CA, Gopalakrishnan M and Malysz J (2007) Distinct profiles of {alpha}7 nAChR positive allosteric modulation revealed by structurally diverse chemotypes. *Mol Pharmacol* **72**(3):715-724.

Halevi S, McKay J, Palfreyman M, Yassin L, Eshel M, Jorgensen E and Treinin M (2002) The C. elegans ric-3 gene is required for maturation of nicotinic acetylcholine receptors. *EMBO J* **21**(5):1012-1020.

Haydar SN and Dunlop J (2010) Neuronal nicotinic acetylcholine receptors - targets for the development of drugs to treat cognitive impairment associated with schizophrenia and Alzheimer's disease. *Curr Top Med Chem* **10**(2):144-152.

Horenstein NA, Leonik FM and Papke RL (2008) Multiple pharmacophores for the selective activation of nicotinic alpha7-type acetylcholine receptors. *Mol Pharmacol* **74**(6):1496-1511.

Hu M, Gopalakrishnan M and Li J (2009) Positive allosteric modulation of alpha7 neuronal nicotinic acetylcholine receptors: lack of cytotoxicity in PC12 cells and rat primary cortical neurons. *Br J Pharmacol* **158**(8):1857-1864.

Jindrichova M, Lansdell SJ and Millar NS (2012) Changes in temperature have opposing effects on current amplitude in alpha7 and alpha4beta2 nicotinic acetylcholine receptors. *PLoS One* **7**(2):e32073.

Johnson J, E. M., Koike T and Franklin J (1992) A "calcium set-point hypothesis" of neuronal dependence on neurotrophic factor. *Exp Neurol* **115**(1):163-166.

Jope RS and Gu X (1991) Seizures increase acetylcholine and choline concentrations in rat brain regions. *Neurochem Res* **16**(11):1219-1226.

Kageyama-Yahara N, Suehiro Y, Yamamoto T and Kadowaki M (2008) IgE-induced degranulation of mucosal mast cells is negatively regulated via nicotinic acetylcholine receptors. *Biochem Biophys Res Commun* **377**(1):321-325.

Land BR, Salpeter EE and Salpeter MM (1981) Kinetic paramenters for acetylcholine interaction in intact neuromuscular junction. *Proc Natl Acad Sci USA* **78**(11):7200-7204.

Li P and Steinbach JH (2010) The neuronal nicotinic alpha4beta2 receptor has a high maximal probability of being open. *Br J Pharm* **160**(8):1906-1915.

Li Y, Papke RL, He Y-J, Millard B and Meyer EM (1999) Characterization of the neuroprotective and toxic effects of α7 nicotinic receptor activation in PC12 cells. *Brain Res* **81**(4):218-225.

Lopez-Hernandez G, Placzek AN, Thinschmidt JS, Lestage P, Trocme-Thibierge C, Morain P and Papke RL (2007) Partial agonist and neuromodulatory activity of S 24795 for alpha7 nAChR responses of hippocampal interneurons. *Neuropharmacology* **53**(1):134-144.

Lukas RJ, Lucero L, Buisson B, Galzi JL, Puchacz E, Fryer JD, Changeux JP and Bertrand D (2001) Neurotoxicity of channel mutations in heterologously expressed alpha7-nicotinic acetylcholine receptors. *Eur J Neurosci* **13**(10):1849-1860.

Mansvelder HD and McGehee DS (2000) Long-term potentiation of excitatory inputs to brain reward areas by nicotine. *Neuron* **27**(2):349-357.

Marrero MB and Bencherif M (2009) Convergence of alpha 7 nicotinic acetylcholine receptor-activated pathways for anti-apoptosis and anti-inflammation: central role for JAK2 activation of STAT3 and NF-kappaB. *Brain Res* **1256**:1-7.

Ng HJ, Whittemore ER, Tran MB, Hogenkamp DJ, Broide RS, Johnstone TB, Zheng L, Stevens KE and Gee KW (2007) Nootropic alpha7 nicotinic receptor allosteric modulator derived from GABAA receptor modulators. *Proc Natl Acad Sci U S A* **104**(19):8059-8064.

Orr-Urtreger A, Broide RS, Kasten MR, Dang H, Dani JA, Beaudet AL and Patrick JW (2000) Mice homozygous for the L250T mutation in the alpha7 nicotinic acetylcholine receptor show increased neuronal apoptosis and die within 1 day of birth. *J Neurochem* **74**(5):2154-2166.

Palma E, Bertrand S, Binzoni T and Bertrand D (1996) Neuronal nicotinic alpha 7 receptor expressed in Xenopus oocytes presents five putative binding sites for methyllycaconitine. *J Physiol* **491**:151-161.

Papke RL (2009) Tricks of Perspective: Insights and limitations to the study of macroscopic currents for the analysis of nAChR activation and desensitization. *Journal of Molecular Neuroscience* **40**(1-2):77-86.

Papke RL, Bencherif M and Lippiello P (1996) An evaluation of neuronal nicotinic acetylcholine receptor activation by quaternary nitrogen compounds indicates that choline is selective for the α7 subtype. *Neurosci Lett* **213**:201-204.

Papke RL, Kem WR, Soti F, López-Hernández GY and Horenstein NA (2009) Activation and desensitization of nicotinic alpha7-type acetylcholine receptors by benzylidene anabaseines and nicotine. *J Pharmacol Exp Ther* **329**(2):791-807.

Papke RL, Meyer E, Nutter T and Uteshev VV (2000a) Alpha7-selective agonists and modes of alpha7 receptor activation. *Eur J Pharmacol* **393**(1-3):179-195.

Papke RL and Papke JKP (2002) Comparative pharmacology of rat and human alpha7 nAChR conducted with net charge analysis. *Br J of Pharm* **137**(1):49-61.

Papke RL, Sanberg PR and Shytle RD (2001) Analysis of mecamylamine stereoisomers on human nicotinic receptor subtypes. *J Pharmacol Exp Ther* **297**(2):646-656.

Papke RL and Thinschmidt JS (1998) The correction of alpha7 nicotinic acetylcholine receptor concentration-response relationships in *Xenopus* oocytes. *Neurosci Let* **256**:163-166.

Papke RL, Webster JC, Lippiello PM, Bencherif M and Francis MM (2000b) The activation and inhibition of human nAChR by RJR-2403 indicate a selectivity for the α4β2 receptor subtype. *J Neurochem* **75**:204-216.

Parrish WR, Rosas-Ballina M, Gallowitsch-Puerta M, Ochani M, Ochani K, Yang LH, Hudson L, Lin X, Patel N, Johnson SM, Chavan S, Goldstein RS, Czura CJ, Miller EJ, Al-Abed Y, Tracey KJ and Pavlov VA (2008) Modulation of TNF release by choline requires alpha7 subunit nicotinic acetylcholine receptor-mediated signaling. *Mol Med* **14**(9-10):567-574.

Pavlov VA, Ochani M, Yang LH, Gallowitsch-Puerta M, Ochani K, Lin X, Levi J, Parrish WR, Rosas-Ballina M, Czura CJ, Larosa GJ, Miller EJ, Tracey KJ and Al-Abed Y (2007) Selective alpha7-nicotinic acetylcholine receptor agonist GTS-21 improves survival in murine endotoxemia and severe sepsis. *Crit Care Med* **35**(4):1139-1144.

Press WH (1988) *Numerical Recipies in C: The art of Scientific Computing*. Cambridge University Press, Cambridge, United Kingdom.

Scremin OU and Jenden DJ (1991) Time-dependent changes in cerebral choline and acetylcholine induced by transient global ischemia in rats. *Stroke* **22**(5):643-647.

Seguela P, Wadiche J, Dinely-Miller K, Dani JA and Patrick JW (1993) Molecular cloning, functional properties and distribution of rat brain alpha 7: a nicotinic cation channel highly permeable to calcium. *J Neurosci* **13(2)**:596-604.

Sitzia F, Brown JT, Randall AD and Dunlop J (2011) Voltage- and Temperature-Dependent Allosteric Modulation of alpha7 Nicotinic Receptors by PNU120596. *Front Pharmacol* **2**:81.

Suzuki T, Hide I, Matsubara A, Hama C, Harada K, Miyano K, Andra M, Matsubayashi H, Sakai N, Kohsaka S, Inoue K and Nakata Y (2006) Microglial alpha7 nicotinic acetylcholine receptors drive a phospholipase C/IP3 pathway and modulate the cell activation toward a neuroprotective role. *J Neurosci Res* **83**(8):1461-1470.

Thomsen MS, Hansen HH, Timmerman DB and Mikkelsen JD (2010) Cognitive improvement by activation of alpha7 nicotinic acetylcholine receptors: from animal models to human pathophysiology. *Curr Pharm Des* **16**(3):323-343.

Treinin M (2008) RIC-3 and nicotinic acetylcholine receptors: biogenesis, properties, and diversity. *Biotechnol J* **3**(12):1539-1547.

Uteshev VV, Meyer EM and Papke RL (2002) Activation and inhibition of native neuronal alpha-bungarotoxin-sensitive nicotinic ACh receptors. *Brain Res* **948**(1-2):33-46.

Uteshev VV, Meyer EM and Papke RL (2003) Regulation of neuronal function by choline and 4OH-GTS-21 through alpha7 nicotinic receptors. *J Neurophysiol* **89**(4):33-46.

van Westerloo DJ, Giebelen IA, Florquin S, Bruno MJ, Larosa GJ, Ulloa L, Tracey KJ and van der Poll T (2006) The vagus nerve and nicotinic receptors modulate experimental pancreatitis severity in mice. *Gastroenterology* **130**(6):1822-1830.

Williams DK, Stokes C, Horenstein NA and Papke RL (2011a) The effective opening of nicotinic acetylcholine receptors with single agonist binding sites. *J Gen Physiol* **137**(4):369-384.

Williams DK, Wang J and Papke RL (2011b) Investigation of the Molecular Mechanism of the Alpha7 nAChR Positive Allosteric Modulator PNU-120596 Provides Evidence for Two Distinct Desensitized States. *Mol Pharmacol* **80**(6):1013-1032.

Williams DK, Wang J and Papke RL (2011c) Positive allosteric modulators as an approach to nicotinic acetylcholine receptor-targeted therapeutics: Advantages and limitations. *Biochem Pharmacol* **82**(8):915-930.

Wooltorton JR, Pidoplichko VI, Broide RS and Dani JA (2003) Differential desensitization and distribution of nicotinic acetylcholine receptor subtypes in midbrain dopamine areas. *J Neurosci* **23**(8):3176-3185.

Young GT, Zwart R, Walker AS, Sher E and Millar NS (2008) Potentiation of alpha7 nicotinic acetylcholine receptors via an allosteric transmembrane site. *Proc Natl Acad Sci U S A* **105**(38):14686-14691.

Molecular Pharmacology Fast Forward. Published on July 24, 2012 as DOI: 10.1124/mol.112.080317
This article has not been copyedited and formatted. The final version may differ from this version.

Footnotes

Dustin K. Williams and Can Peng contributed equally.

This work was supported by National Institute of Health grants [RO1-GM57481] and [T32-AG000196], and by a Florida Biomedical James and Esther King Research grant [KG12].

Molecular Pharmacology Fast Forward. Published on July 24, 2012 as DOI: 10.1124/mol.112.080317
This article has not been copyedited and formatted. The final version may differ from this version.

Figure legends

Figure 1. A) Representative currents illustrating the varying shapes of responses at different concentrations of ACh contrasted with responses to 300 μM ACh and B) the concentration-response relationship for whole-cell peak currents and net charge responses evoked by ACh. The curve for net charge was fit between 1 μM ACh and 300 μM ACh, denoted by the solid grey boxes. Each point represents the mean ± SEM from 4-8 cells. Net charge responses were calculated for a period of 1 s following ACh application.

Figure 2. Saturation binding of [^{125}I] α-btx binding to intact A7R3HC10 cells. A) No specific binding was detected with untransfected HEK 293. Values are the mean ± SEM of 5-6 replicates. B) A saturation binding curve from one representative experiment. C) A Scatchard transformation of the same data. The average K_d and B_{max} values from three independent saturation binding experiments are 1000 ± 70 pM and 7.7 x 10^{-8} ± 1.3 x 10^{-8} pmol/cell, respectively. Specific binding is defined as the difference between total binding and non-specific binding. Non-specific binding was determined using 1 μM unlabeled α-btx.

Figure 3. Representative whole-cell currents from A7R3HC10 cells evoked by 3 second co-applications of either 1 mM ACh or 100 μM ACh in combination with 10 μM PNU-120596.

Figure 4. Effects of PNU-120596 PNU and choline on the survival of A7R3HC10 cells. The cytotoxicity profile of 0-30 μM PNU-120596 with 0-3 mM choline when treatments were incubated at 37 °C with 5% CO_2. The * indicates a two-tailed p-value <0.05. Each value is the average ± SEM of 3-5 independent experiments. Two sets of cells were plated from the same passage one day prior to experiments. Untransfected HEK 293 cells were treated in parallel and were unaffected by all choline and PNU-120596 treatments (data not shown).

Figure 5. Temperature dependence of PNU-120596 on potentiation of α7-mediated responses. Whole-cell currents from A7R3HC10 cells evoked by 3-second co-application of 100 μM ACh and 10 μM or 1 μM PNU-120596 were recorded every 60 seconds with varied temperatures between 23.5 °C and 37 °C. A) Time course for 100 μM ACh and 10 μM PNU-120596 evoked peak responses (black circles, n=8). Temperature is indicated by gray squares. B) Representative traces of 100 μM ACh and

Molecular Pharmacology Fast Forward. Published on July 24, 2012 as DOI: 10.1124/mol.112.080317
This article has not been copyedited and formatted. The final version may differ from this version.

10 μM PNU-120596 evoked responses recorded at the indicated temperature. C) Time course for 100 μM ACh and 1 μM PNU-120596 evoked peak responses (black circles, n=9). Temperature is indicated by gray squares. D) Representative traces of 100 μM ACh and 1 μM PNU-120596 evoked responses recorded at the indicated temperature. Responses were normalized to the average peak amplitude of the three initial responses obtained at 23.5 °C. Each data point is represented as the average normalized value ± SEM.

Figure 6. PNU-120596 cytotoxicity measured at 28°C. A) Cytotoxicity profile of 0-30 μM PNU-120596 with 0-3 mM choline when treatments were incubated at 28°C with 5% CO_2. The * indicates a two-tailed p-value <0.05. Each value is the average ± SEM of 3-5 independent experiments. Sets of cells were plated from the same passage one day prior to experiments as the cells illustrated in Figure 4. Untransfected HEK 293 cells were treated in parallel and were unaffected by all choline and PNU-120596 treatments at 28°C and 37 °C (data not shown).

Figure 7. Sensitivity of the cytotoxic effect of 100 μM choline and 10 μM PNU-120596 co-treatment in HBSS at 28°C to the competitive antagonist MLA. Either 10 nM or 100 nM MLA was added at the time indicated, relative to the toxic 100 μM choline and 10 μM PNU-120596 co-treatment. The * indicates a two-tailed p-value <0.05. Values are averages ± SEM from 3 independent experiments.

Figure 8. Elimination of the temperature-dependence of PNU-120596 cytotoxicity. A) Cytotoxicity of 0 – 3 mM choline and 10 μM PNU-120596 treatments at 28°C with 5% CO_2 in HBSS solutions with 10% FBS. B) Cytotoxicity of 0 – 3 mM choline and 10 μM PNU-120596 treatments at 37 °C with 5% CO_2 in HBSS solutions with 10% FBS. Notably, a factor in FBS appears to remove the apparent temperature-dependent cytotoxicity in Figure 9. C) Cytotoxicity of 0 – 3 mM choline and 10 μM PNU-120596 treatments at 28°C with 5% CO_2 in HBSS solutions with 30 μM BSA. D) Cytotoxicity of 0 – 3 μM choline and 10 μM PNU-120596 treatments at 37 °C with 5% CO_2 in HBSS solutions with 30 μM BSA. The effect of 30 μM BSA appears to be very similar to that of FBS. The * indicates a two-tailed p-value < 0.05. Values are averages ± SEM from 3 independent experiments.

Figure 9. Sensitivity of the cytotoxic effect of 100 μM choline and 10 μM PNU-120596 co-treatment in HBSS with 30 μM BSA at 37 °C to the competitive antagonist MLA and

Molecular Pharmacology Fast Forward. Published on July 24, 2012 as DOI: 10.1124/mol.112.080317
This article has not been copyedited and formatted. The final version may differ from this version.

the non-competitive antagonist mecamylamine. 10 nM and 100 nM MLA or 10 μM and 100 μM mecamylamine were added at the time indicated, relative to the toxic 100 μM choline and 10 μM PNU-120596 co-treatment. The * indicates a two-tailed p-value < 0.05. Values are averages ± SEM from 3 independent experiments.

Figure 10. Partial preservation of PNU-120596 potentiation at 37 °C in external solution containing 30 μM BSA. A) Whole-cell recordings from A7R3HC10 cells evoked by 3 second co-application of 100 μM ACh and 10 μM PNU-120596 in the absence or presence of 30 μM BSA with varied temperatures between 23.5 °C and 37 °C. Data in the absence of BSA are the same as those shown in Figure 5A. Responses were normalized to the average peak amplitude of the three initial responses obtained at 23.5 °C. Data in the presence of BSA were represented as the average normalized value ± SEM of 11 cells. B) Data from the same cells in panel A were shown as the average absolute peak amplitude ± SEM. C) Representative traces of 100 μM ACh and 10 μM PNU-120596 evoked responses in the presence of 30 μM BSA recorded at the indicated temperature.

Molecular Pharmacology Fast Forward. Published on July 24, 2012 as DOI: 10.1124/mol.112.080317
This article has not been copyedited and formatted. The final version may differ from this version.

Table 1. 10-90% rise-times and rise-slopes with increasing concentrations of ACh.

[ACh], μM	10-90% Rise-time (ms)	10-90% Rise-slope (pA/ms)
30	74.6 ± 30.8	0.195 ± 0.081
100	22.3 ± 7.20	1.34 ± 0.465
300	9.86 ± 1.45	22.7 ± 6.90
1000	2.61 ± 0.259	47.2 ± 12.4
3000	1.84 ± 0.53	294 ± 105

Table 2. Summary of the observed temperature effects on α7 PAM activity from whole-cell electrophysiology experiments.

Drug	Average absolute value (pA)		Normalized to average peak at 23.5 ˚C
	23.5 ˚C	37 ˚C	37 ˚C
1 mM ACh (n=7)	643 ± 132	294 ± 55	0.474 ± 0.032
Type I PAM			
100 μM ACh and 1 mM 5-HI (n=12)	-1346 ± 158	-455 ± 70	0.330 ± 0.024
100 μM ACh and 10 μM NS-1738 (n=6)	-3602 ± 294	-1244 ± 276	0.339 ± 0.052
Type II PAM			
100 μM ACh and 10 μM PNU-120596 in ES (n=8)	-1333 ± 414	-104 ± 31	0.117 ± 0.028
100 μM ACh and 1 μM PNU-120596 in ES (n=9)	-509 ± 136	-44 ± 7	0.129 ± 0.029
100 μM ACh and 10 μM PNU-120596 in ES^{BSA} (n=11)	-2753 ± 284**	-392 ± 97*	0.148 ± 0.030
100 μM ACh and 10 μM TQS (n=7)	-3080 ± 484	-1438 ± 229	0.464 ± 0.025

ES, external solution

ES^{BSA}, external solution containing 30 μM BSA

** P<0.01. The effect of 30 μM BSA in external solution to increase the 100 μM ACh and 10 μM PNU-120596 response at 23.5 ˚C is statistically significant by comparing the average responses from 11 cells recorded in ES^{BSA} to the average responses of 8 cells recorded in ES.

* P<0.05. The effect of 30 μM BSA in external solution to increase the 100 μM ACh and 10 μM PNU-120596 response at 37 ˚C is statistically significant by comparing the average responses from 11 cells recorded in ES^{BSA} to the average responses of 8 cells recorded in ES.

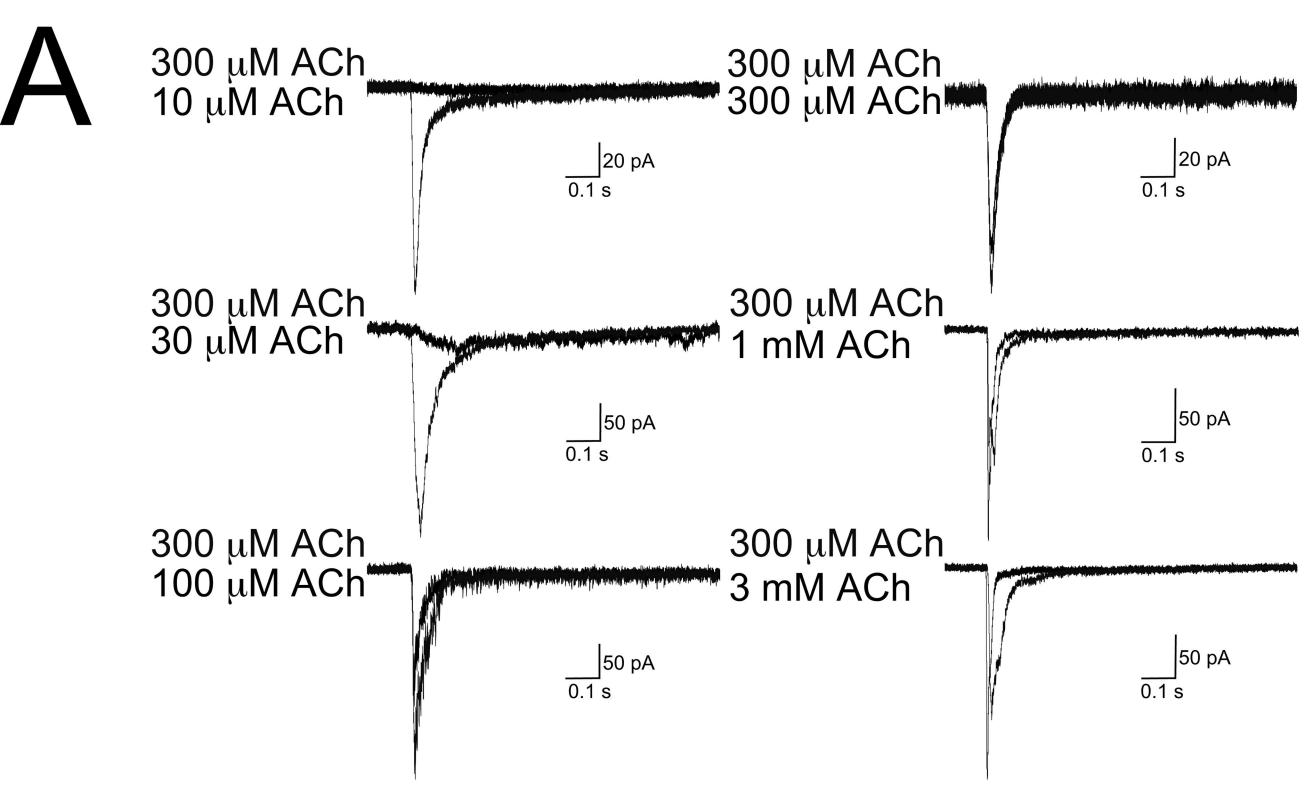
A
300 μM ACh
10 μM ACh
20 pA
0.1 s
300 μM ACh
300 μM ACh
20 pA
0.1 s
300 μM ACh
30 μM ACh
50 pA
0.1 s
300 μM ACh
1 mM ACh
50 pA
0.1 s
300 μM ACh
100 μM ACh
50 pA
0.1 s
300 μM ACh
3 mM ACh
50 pA
0.1 s

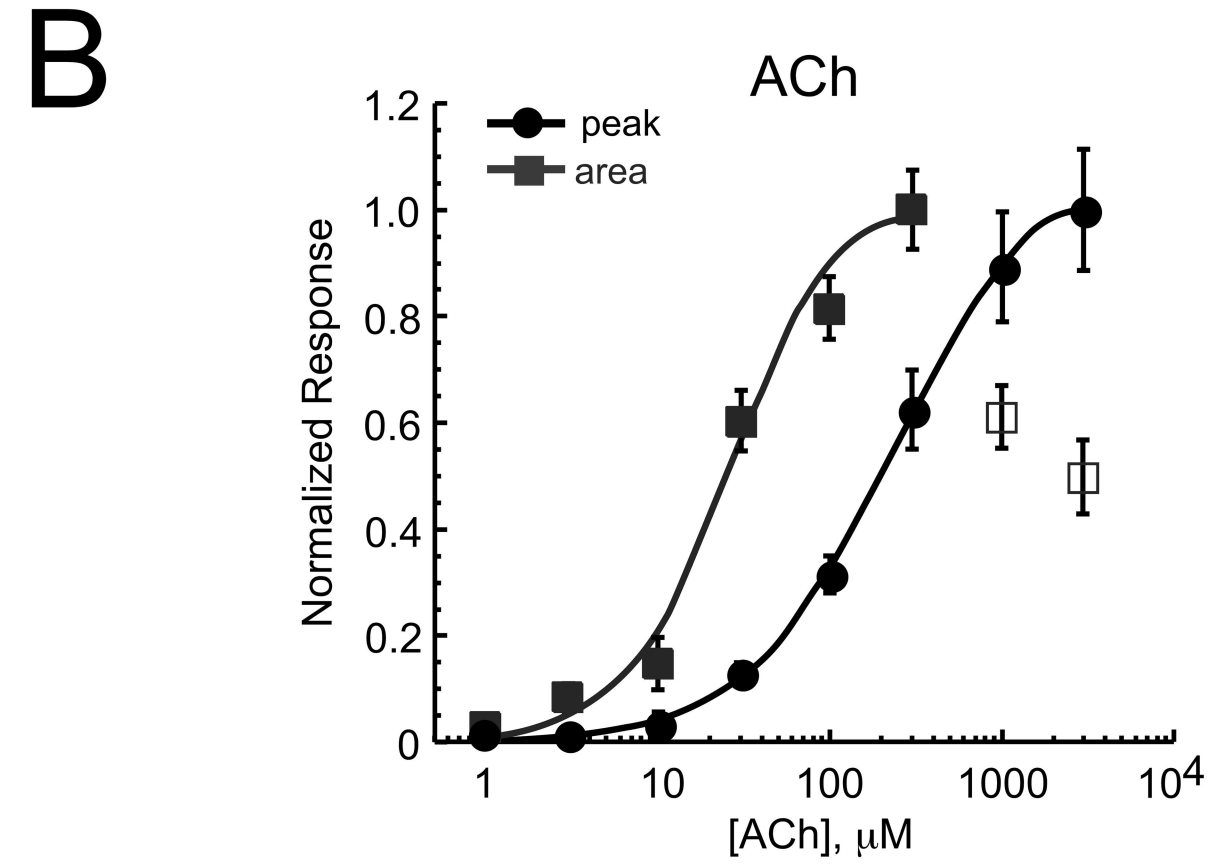
B
ACh
peak
area
Normalized Response
1.2
1.0
0.8
0.6
0.4
0.2
0
1
10
100
1000
10^4
[ACh], μM

Figure 1

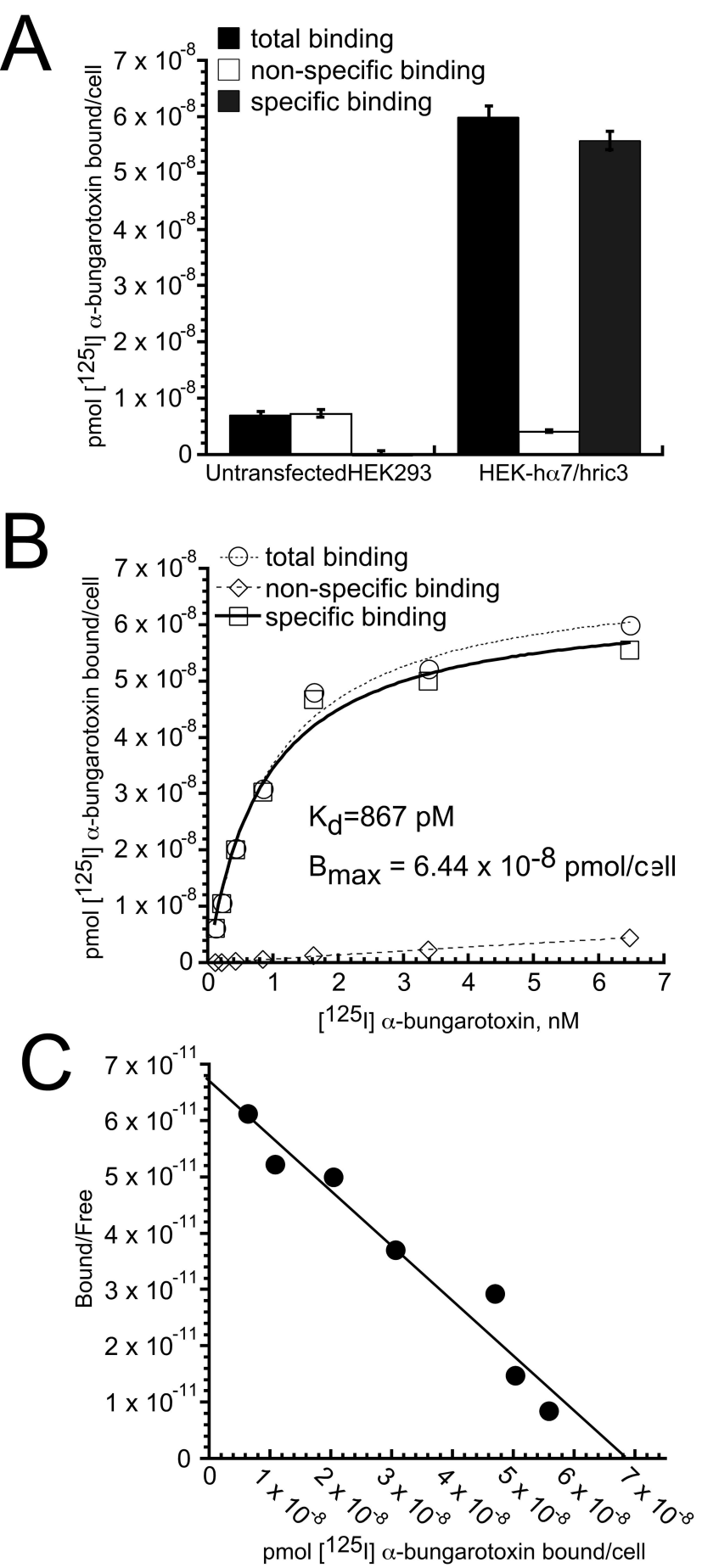
A
total binding
non-specific binding
specific binding
pmol [125I] α-bungarotoxin bound/cell
7 x 10-8
6 x 10-8
5 x 10-8
4 x 10-8
3 x 10-8
2 x 10-8
1 x 10-8
0
UntransfectedHEK293
HEK-hα7/hric3
B
total binding
non-specific binding
specific binding
pmol [125I] α-bungarotoxin bound/cell
Kd=867 pM
Bmax = 6.44 x 10-8 pmol/cell
0
1
2
3
4
5
6
7
[125I] α-bungarotoxin, nM
C
Bound/Free
7 x 10-11
6 x 10-11
5 x 10-11
4 x 10-11
3 x 10-11
2 x 10-11
1 x 10-11
0
1 x 10-8
2 x 10-8
3 x 10-8
4 x 10-8
5 x 10-8
6 x 10-8
7 x 10-8
pmol [125I] α-bungarotoxin bound/cell

Figure 2

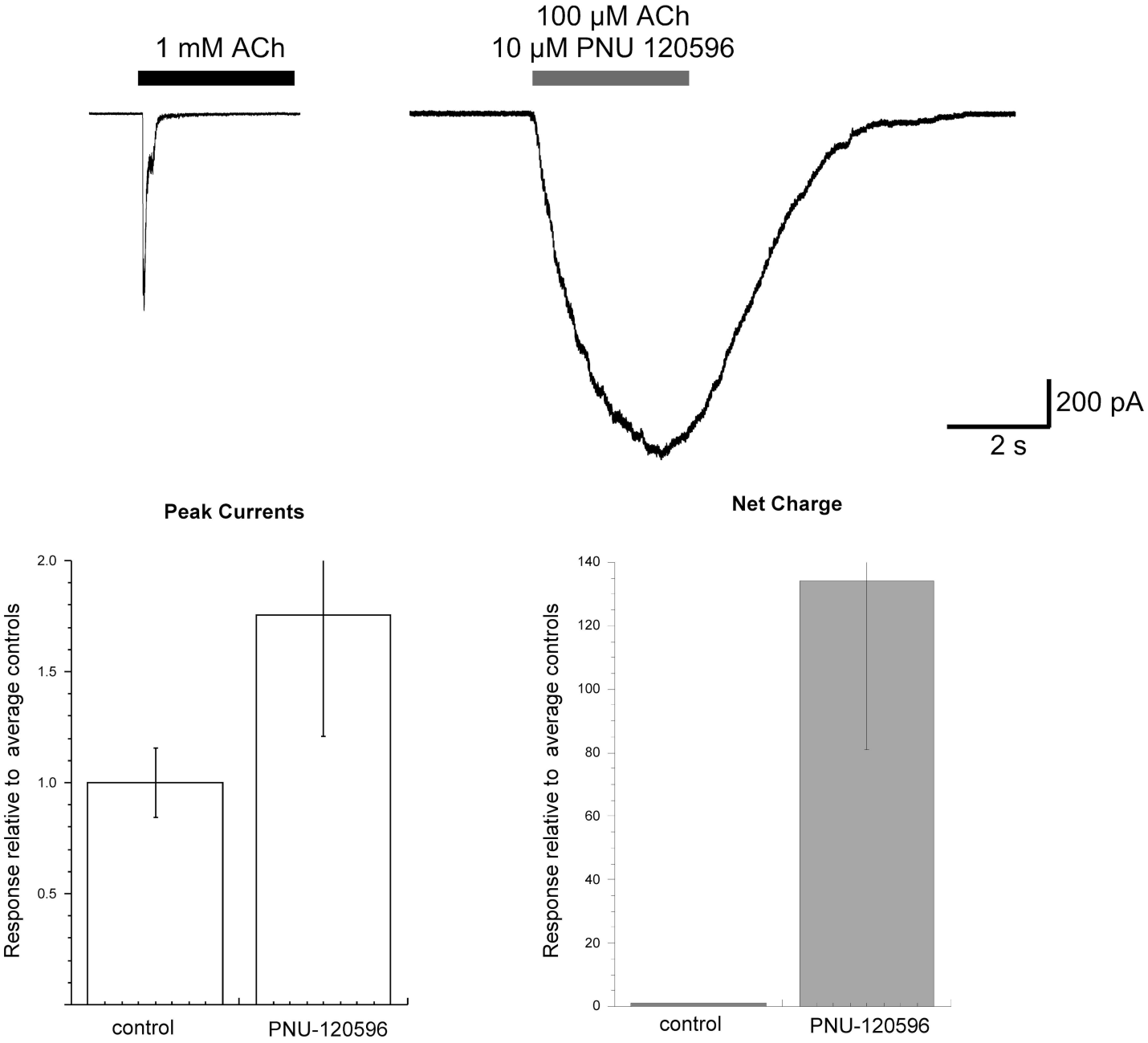
1 mM ACh
100 µM ACh
10 µM PNU 120596
200 pA
2 s
Peak Currents
Response relative to average controls
2.0
1.5
1.0
0.5
control
PNU-120596
Net Charge
Response relative to average controls
140
120
100
80
60
40
20
0
control
PNU-120596

Figure 3

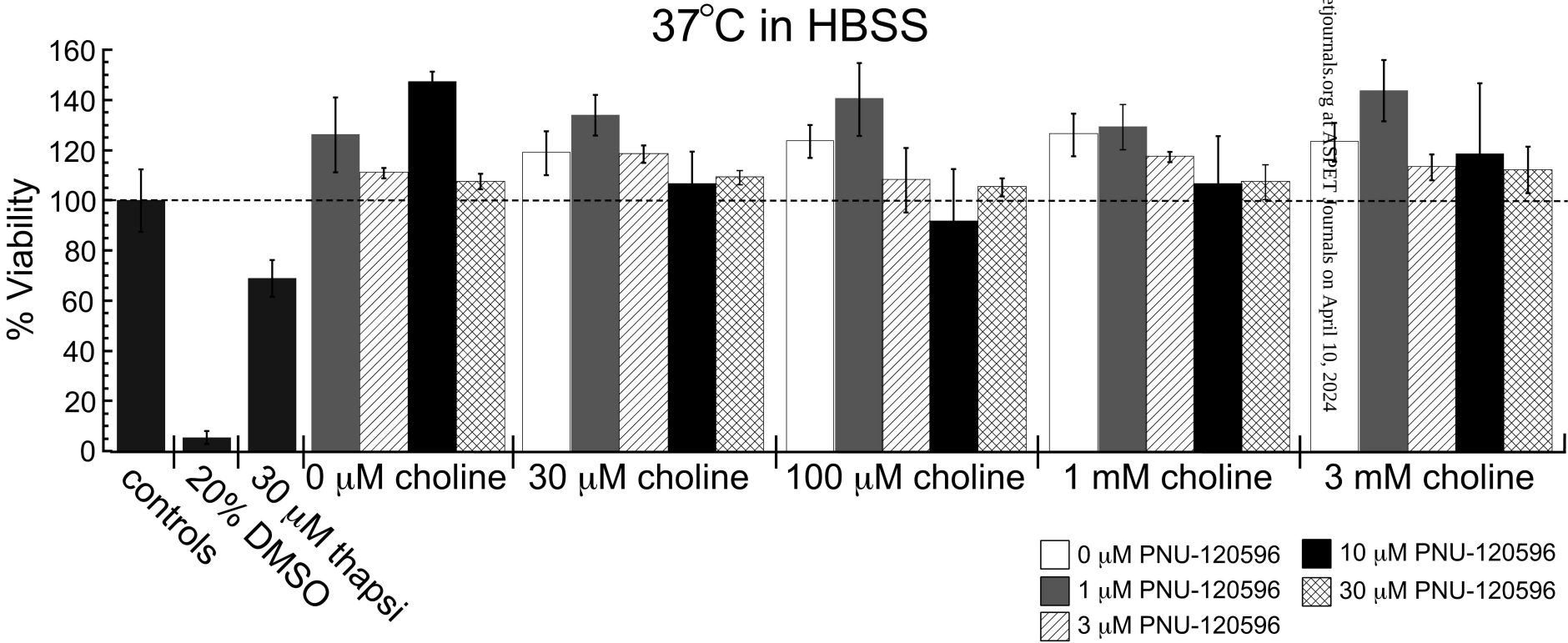

Figure 4

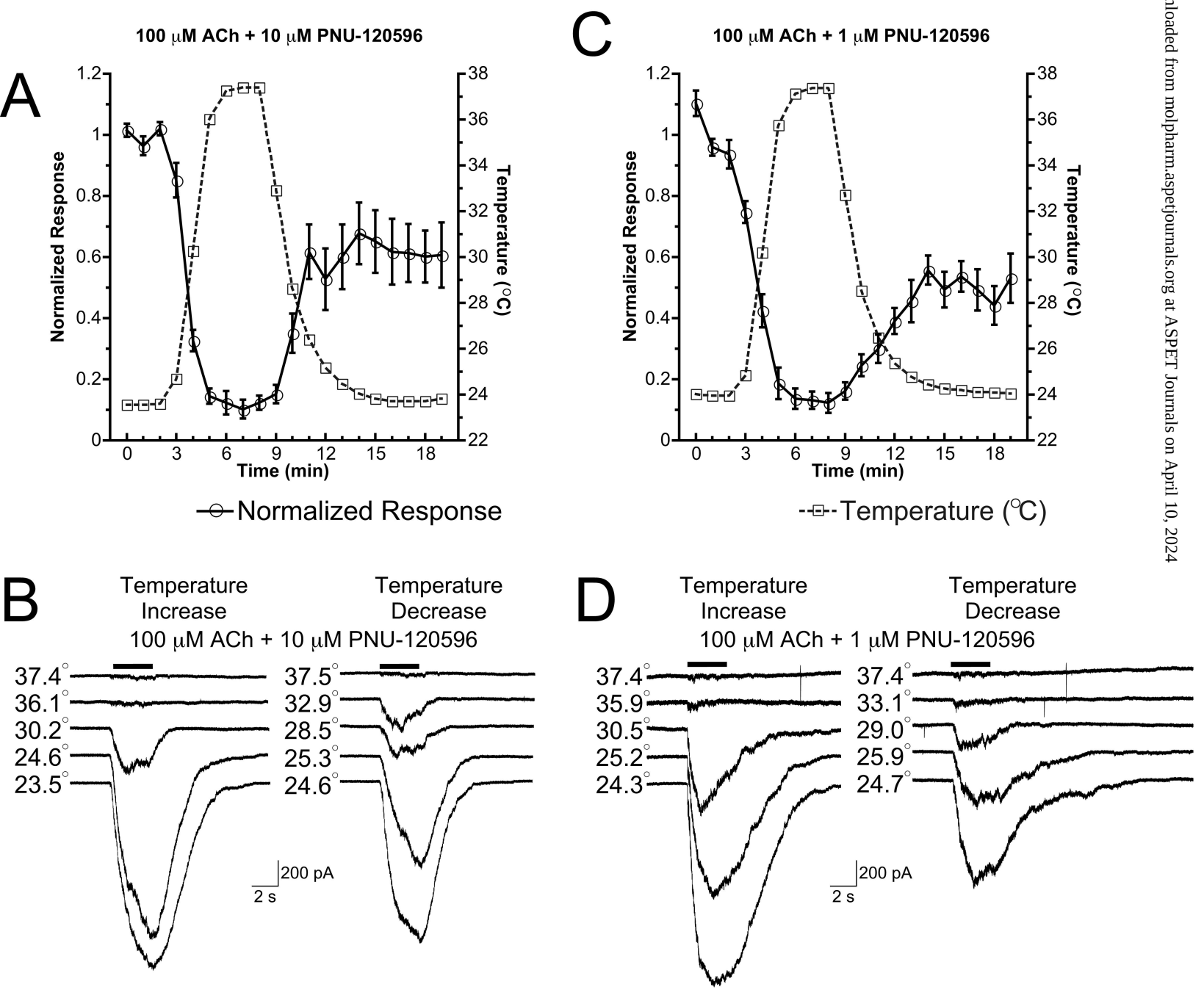

Figure 5

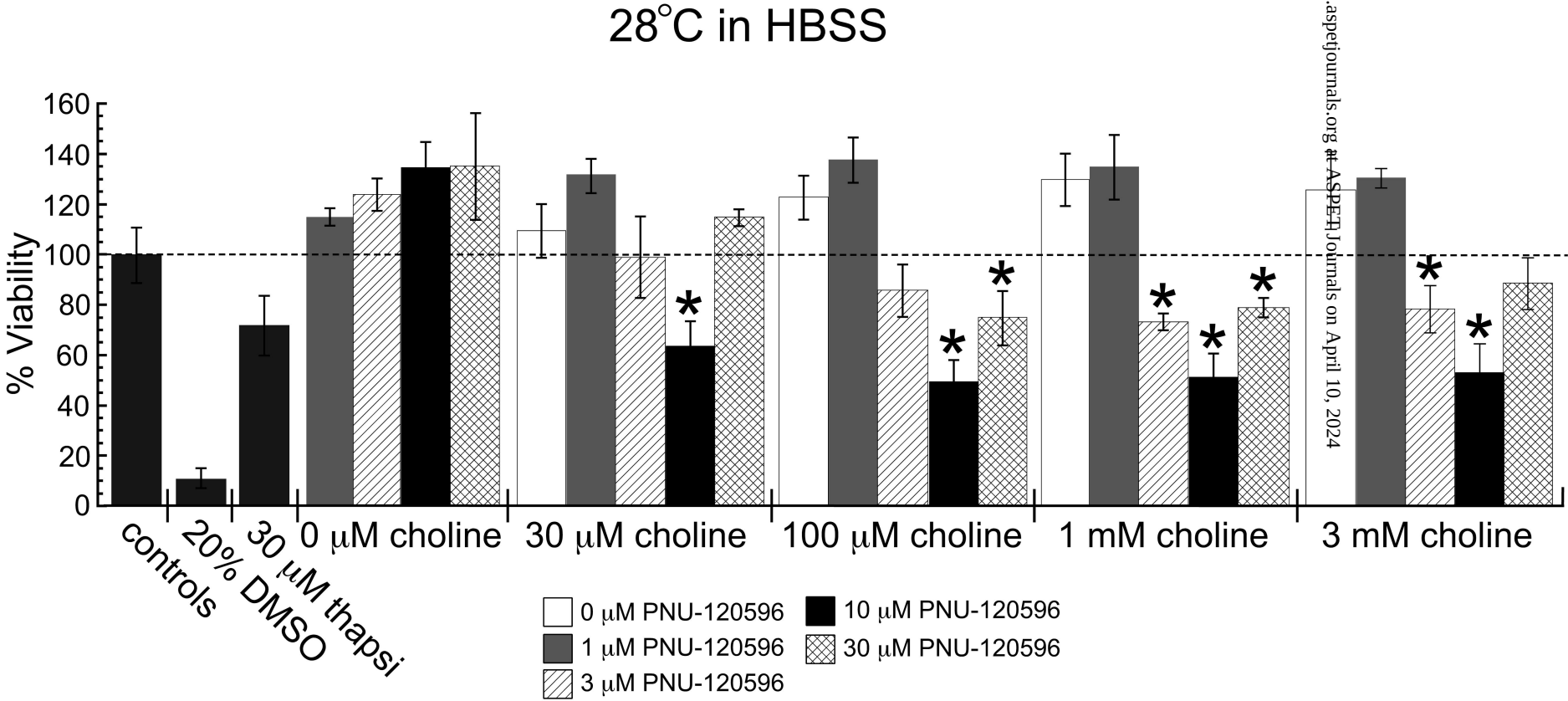

Figure 6

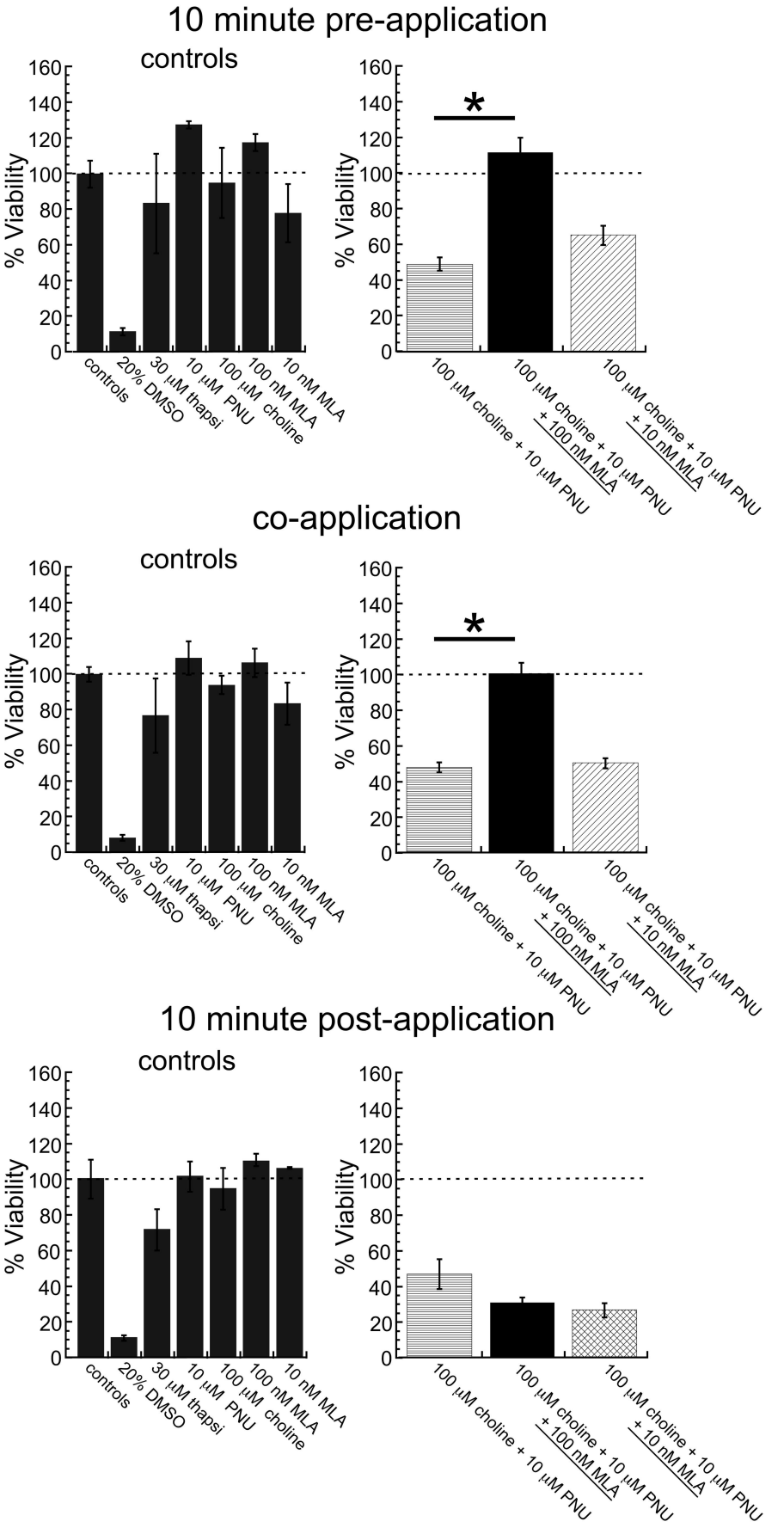
10 minute pre-application
controls
% Viability
160
140
120
100
80
60
40
20
0
controls
20% DMSO
30 μM thapsi
10 μM PNU
100 μM choline
100 nM MLA
10 nM MLA
*
100 μM choline + 10 μM PNU
100 μM choline + 10 μM PNU + 100 nM MLA
100 μM choline + 10 μM PNU + 10 nM MLA
co-application
controls
% Viability
*
100 μM choline + 10 μM PNU
100 μM choline + 10 μM PNU + 100 nM MLA
100 μM choline + 10 μM PNU + 10 nM MLA
10 minute post-application
controls
% Viability
100 μM choline + 10 μM PNU
100 μM choline + 10 μM PNU + 100 nM MLA
100 μM choline + 10 μM PNU + 10 nM MLA

Figure 7

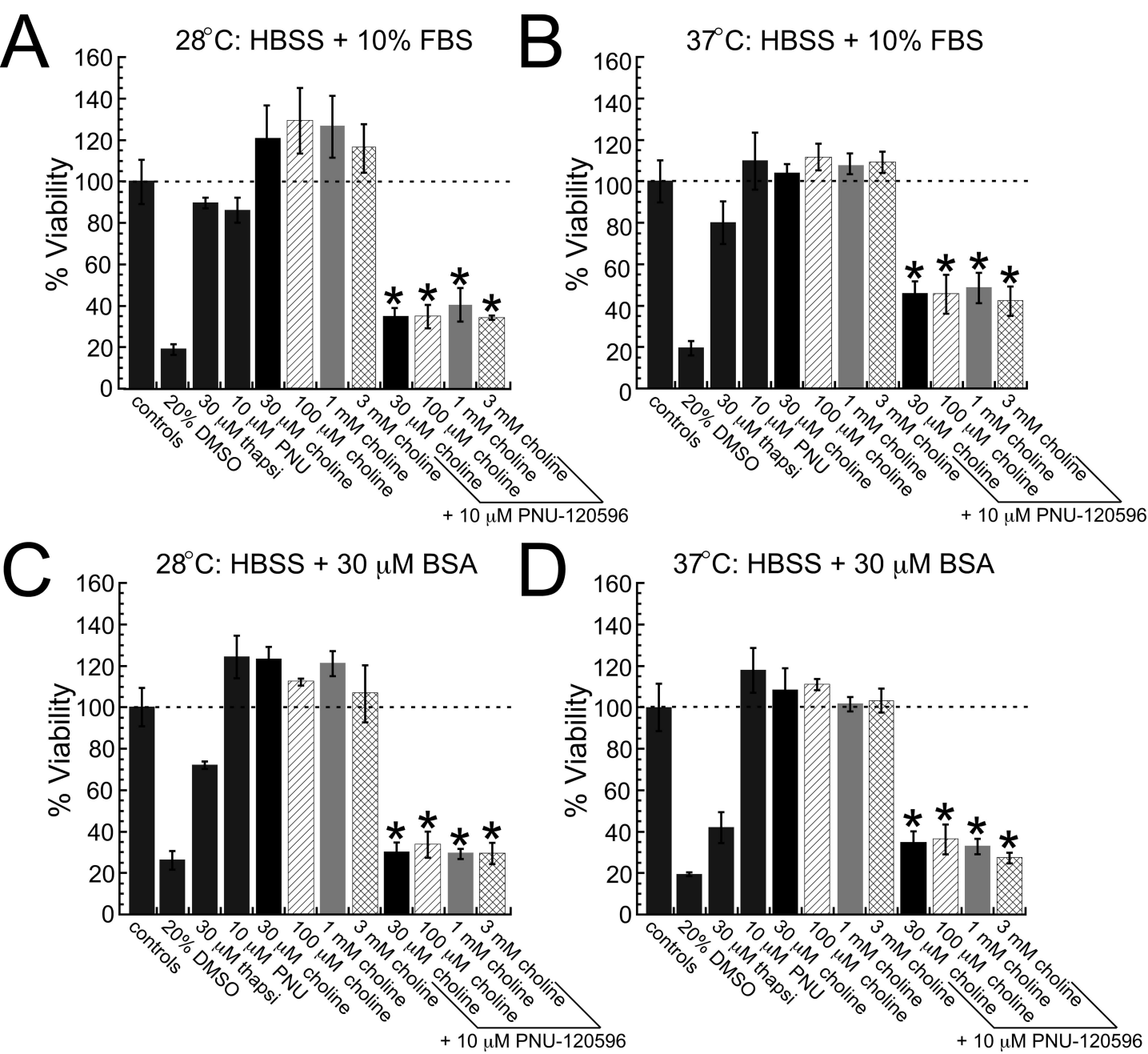
A
28°C: HBSS + 10% FBS
% Viability
controls
20% DMSO
30 μM thapsi
10 μM PNU
30 μM choline
100 μM choline
1 mM choline
3 mM choline
30 μM choline
100 μM choline
1 mM choline
3 mM choline
+ 10 μM PNU-120596
B
37°C: HBSS + 10% FBS
C
28°C: HBSS + 30 μM BSA
D
37°C: HBSS + 30 μM BSA

Figure 8

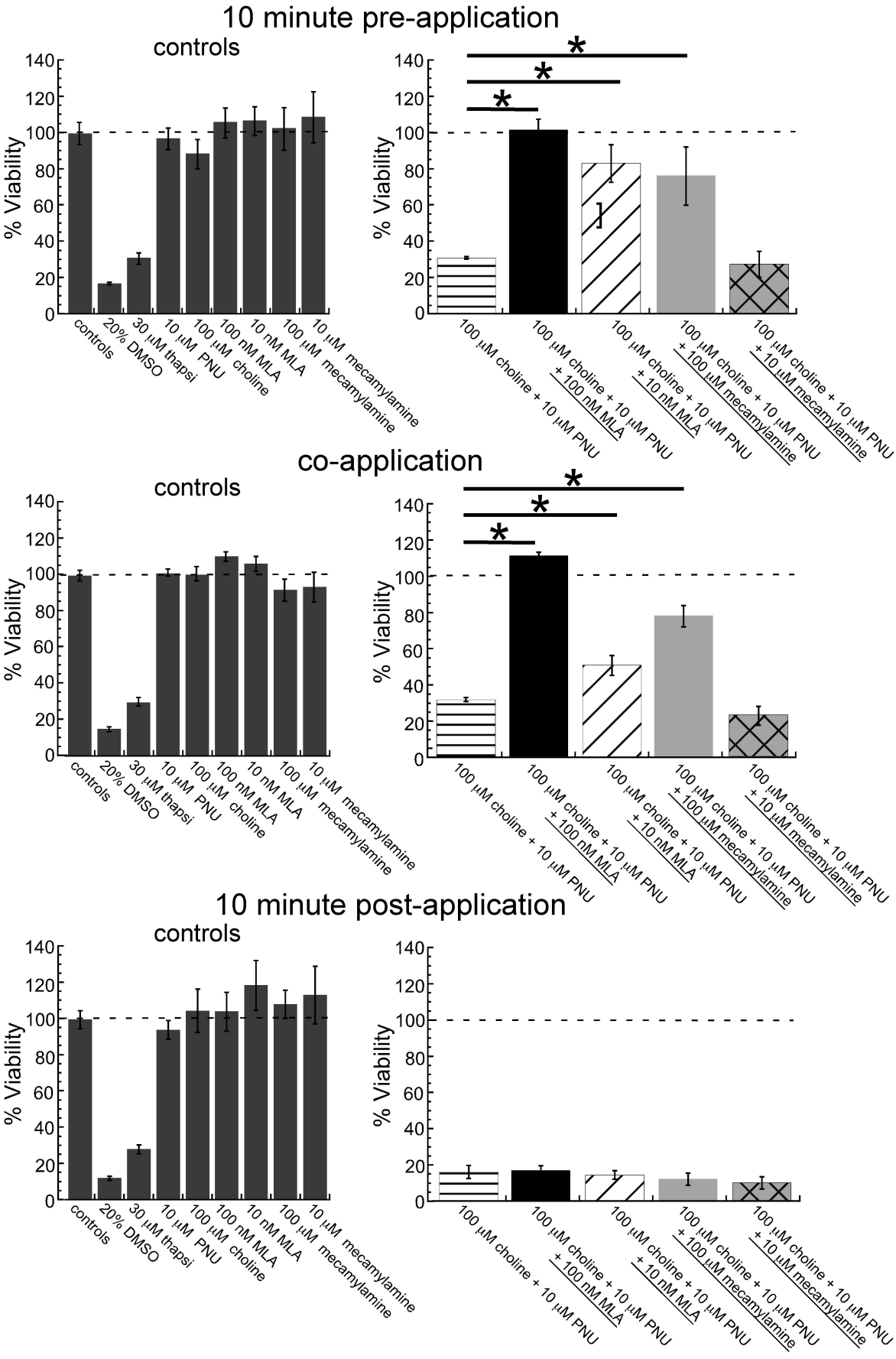
10 minute pre-application
controls
% Viability
controls
20% DMSO
30 μM thapsi
10 μM PNU
100 μM choline
100 nM MLA
10 nM MLA
100 μM mecamylamine
10 μM mecamylamine
100 μM choline + 10 μM PNU
100 μM choline + 10 μM PNU + 100 nM MLA
100 μM choline + 10 μM PNU + 10 nM MLA
100 μM choline + 10 μM PNU + 100 μM mecamylamine
100 μM choline + 10 μM PNU + 10 μM mecamylamine
co-application
10 minute post-application

Figure 9

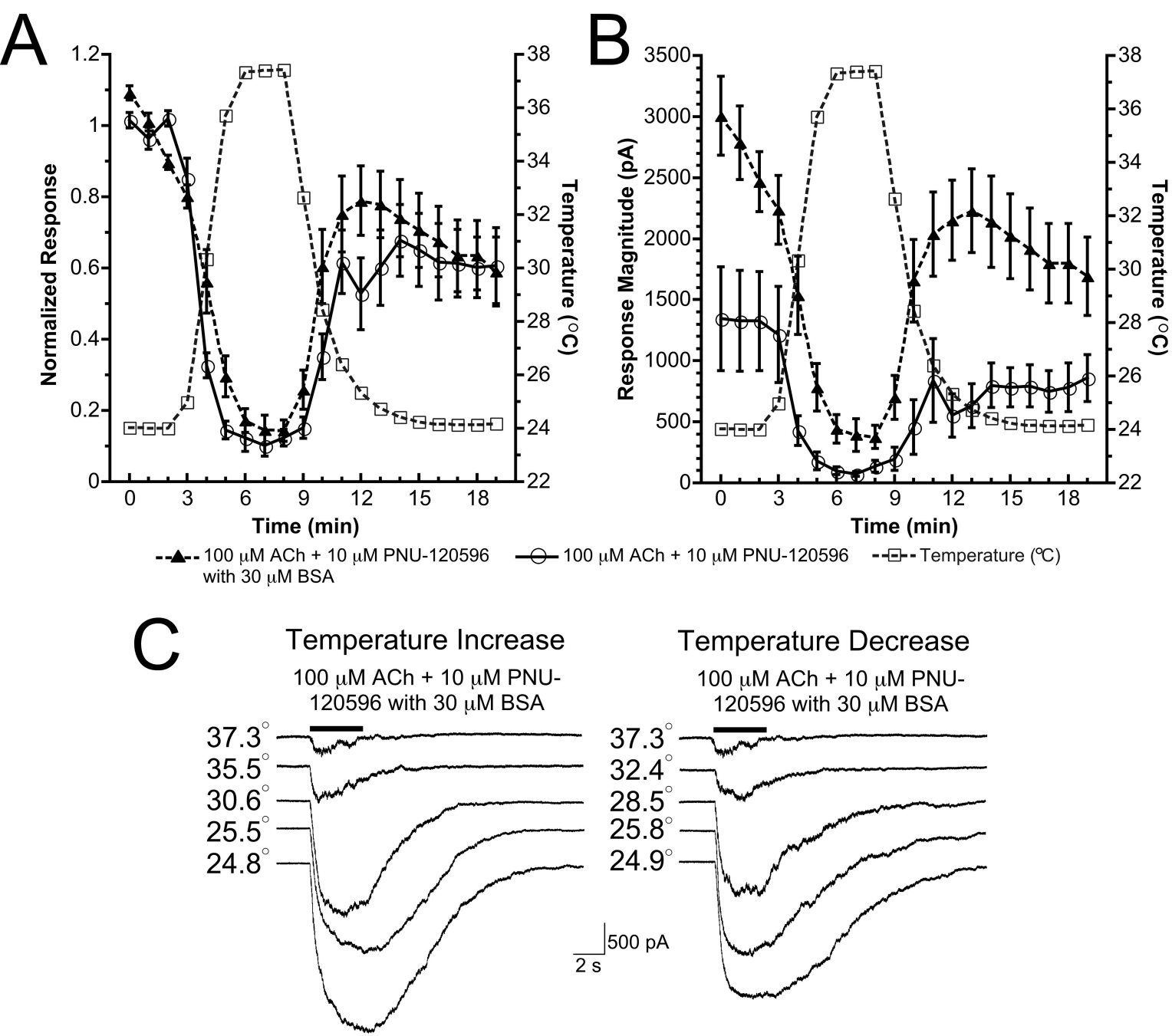
A
B
C
Normalized Response
Response Magnitude (pA)
Temperature (°C)
Time (min)
100 μM ACh + 10 μM PNU-120596 with 30 μM BSA
100 μM ACh + 10 μM PNU-120596
Temperature (°C)
Temperature Increase
Temperature Decrease
100 μM ACh + 10 μM PNU-120596 with 30 μM BSA
37.3°
35.5°
30.6°
25.5°
24.8°
32.4°
28.5°
25.8°
24.9°
500 pA
2 s

Figure 10

Supplemental data

The intrinsically low open probability of α7 nAChR can be overcome by positive allosteric modulation and serum factors leading to the generation of excitotoxic currents at physiological temperatures.

Dustin K. Williams, Can Peng, Matthew R. Kimbrell, and Roger L. Papke

Molecular Pharmacology

Supplemental Materials and Methods

Generation of HEK 293 cells stably expressing human α7 and human RIC-3

Low passage number HEK 293 cells were obtained from American Type Culture Collection (Manassas, VA). The cells were routinely cultured in Dulbecco's modified eagle medium (DMEM) supplemented with 10% fetal bovine serum (FBS). In order to create a HEK 293 cell line stably expressing human α7 and RIC-3, two rounds of stable transfection were performed. The transfections were performed with Fugene HD (Roche, Indianapolis IN) according to manufacturer's directions. The day before transfection, 125,000 cells were plated in 35 mm dishes. First, cells were transfected with 1 μg (per 35 mm dish) of circular pcDNA3.1 plasmid containing the RIC-3 gene. Several (>20) clones that were resistant to 0.15 mg/ml hygromycin (resistance conferred by pcDNA3.1/RIC-3 vector) after a two-week selection period were isolated using cloning cylinders and expanded. Following the selective period, the hygromycin-resistant cell lines were maintained in normal growth media supplemented with 0.15 mg/mL hygromycin. Total RNA was extracted using the SV Total RNA Isolation System (Promega, Madison, WI) and the expression of hRIC-3 mRNA was determined by reverse transcriptase-polymerase chain reaction (RT-PCR). The upper and lower primers for hRIC-3, respectively, were CCGATTTCCACCTATGATG and GGCTGCTTCTGTCTCCTTC, resulting in an expected product size of 346 base pairs. The upper and lower primers for glyceraldehyde-3-phosphate dehydrogenase (GAPDH), respectively, were ACGGATTTGGTCGTATTGG and TGGCATGGACTGTGGTCAT, resulting in an expected product size of 516 base pairs. RT-PCR products were visualized in gels composed of 0.7% agarose and 1.15%Synergel (Diversified Biotech, Dedham MA) . The process of transfection, selection, cloning, and expansion was repeated using a stable HEK-hRIC-3 expressing cell line as the starting point. The hRIC-3-expressing cell line was transfected with 2 μg of circular pCIneo/hα7 plasmid using Fugene HD (Roche, Indianapolis, IN). The cells were selected during a two-week period using 0.45 mg/mL geneticin and 0.015 mg/mL hygromycin, and thereafter maintained in the same concentration of selective antibiotics. Ten colonies were eventually cloned that were resistant to both hygromycin and geneticin that were also positive for both hRIC-3 and hα7 mRNA by RT-PCR. The upper and lower primers for hα7, respectively, were TGGACGTGGATGAGAAGAA and TTCCCACTAGGTCCCATTC, resulting in an expected product size of 414 base pairs. These cell lines were subsequently screened for functional α7 channel expression through whole-cell patch-clamp electrophysiology. The clone that showed highest functional channel expression and was easiest to patch-

clamp was selected for use in all of the following studies. This clone is referred to as the A7R3HC10 cell line for alpha7RIC-3-expressingHEK-derived Clone10. In addition, cell lines were also created stably expressing human α7 alone. HEK 293 cells were transfected with 2 μg of circular pCiNeo plasmid containing the human α7 gene. Cells were selected during a two-week period of exposure to 0.5 mg/mL geneticin (resistance conferred by pCiNeo/α7 vector), and thereafter were maintained in 0.5 mg/mL geneticin. None of the geneticin-resistant and PCR-positive clones for α7 alone responded to co-applications of ACh and PNU-120596 in patch-clamp electrophysiology experiments. However, responses from these cells were observed when cells stably expressing α7 were transiently transfected with hRIC-3 only (not shown). For normal passaging, cells were dissociated with a trypsin-free solution containing 0.02% EDTA in calcium- and magnesium-free Hank's balanced saline solution (HBSS) to avoid non-selective damage to the α7 nAChRs expressed on the cell surface. For electrophysiology experiments, cells were plated on poly-D-lysine-coated cover slips and were used 1-5 days after plating for experiments.

Immunoprecipitation and western blot

Three days prior to preparing the sample for western blotting, 50,000 cells were plated in a 12-well plate treated with poly-D-lysine. Cells were washed with ice cold 1% phosphate-buffered saline, lysed (lysis buffer, protease inhibitor, and phosphatase inhibitor), scraped off the 12- well plate, and transferred into 1.5 ml tubes. The cells were then sonicated on ice and incubated overnight at 4°C with primary antibody ab848, courtesy of Dr. Cecilia Gotti (University of Milan, Italy). The antigen-antibody complexes were incubated with 50 μl of pre-washed protein A magnetic beads (Millipore, Billerica, MA). After washing, immunoprecipitated protein underwent denaturing elution with sample buffer followed by heating to 80°C for 10 minutes. 40 μl were loaded into each well for SDS-polyacrylamide gel electrophoresis using 10% polyacrylamide, along with 1 μl of MagicMarkXP (Life Technologies, Grand Island, NY).

Protein was transferred overnight at 4°C onto a PVDF membrane. Transfer was confirmed by staining the PVDF membrane with Ponceau-S (Bio-Rad, Hercules, CA) and the gel with coomassie blue. Ponceau-S was removed from the membrane with TBS-T. The membrane was blocked at room temperature with 5% BSA. Overnight incubation at 4°C of the primary antibody ab849 (Dr. Cecilia Gotti) was followed by washing the membrane in TBS-T and incubating it with secondary antibody (Abcam, Cambridge, MA) for one hour at room temperature. After washing again with TBS-T,

Super Signal (Thermo Fisher Scientific, Waltham, MA) was added to visualize the protein using the ChemiXRS+ imaging system (Bio-Rad, Hercules, CA).

Fluorescence Microscopy

Untransfected HEK 293, A7R3HC10 (HEK-hα7/hRIC-3), HEK-hα7, and HEK-hRIC-3 cells were plated on square glass coverslips (Fisher Scientific, Waltham, MA) coated with poly-D-lysine and incubated at 37 °C with 5% CO_2 in DMEM media with 10% FBS containing the appropriate selective antibiotic for 24 hours prior to imaging. Cells were treated with 1 μg/mL (~125 nM) of Alexa488-α-btx (Life Technologies, Grand Island, NY) for 45 minutes at 37 °C with 5% CO_2. For a control, the A7R3HC10 cells were also pre-incubated with 1 mM nicotine, and then 1 μg/mL Alexa488-α-btx was co-applied with 1 mM nicotine. After the incubation, the cells were carefully rinsed 4 times with phosphate-buffered saline to remove any excess Alexa488-α-btx. The cells were then fixed with 4% (v/v) formaldehyde for 15 minutes, and washed 3 more times with phosphate-buffered saline before being mounted on coverslips for imaging using VectaShield (Vector Laboratories, Burlingame, CA) mounting media containing the nuclear stain DAPI. The slides were imaged immediately using an Olympus DSU-IX81 spinning disc confocal microscope. The images were obtained using a Hamamatsu C4742-80-12AG Monochrome CCD Camera.

Supplemental data

Generation and characterization of α7 expression in A7R3HC10 cells

Expression of hRIC-3 and hα7 mRNA in hygromycin- and geneticin- resistant clones

Total mRNA was isolated from each hygromycin- and geneticin-resistant clone and tested for the presence of hRIC-3 and hα7 mRNA through RT-PCR. As expected, untransfected HEK 293 were negative for hRIC-3 and for hα7, but bands corresponding to the expected nucleotide length were observed for both hRIC-3 and hα7 from the antibiotic-resistant cell lines (Supplemental Figure 1A). Messenger RNA for Glyceraldehyde 3-phosphate dehydrogenase, a common housekeeping gene, was probed as a positive control to verify that the RT-PCR protocol was successful in the case that hRIC-3 and hα7 bands were absent.

Identification of the hα7 protein via western blot in antibiotic- resistant clones

No labeling was observed from untransfected HEK 293 cells and cells stably expressing hRIC-3. In contrast, some labeling was observed from cells transfected with hα7 while stronger labeling was seen in cells stably expressing both hα7 and hRIC-3 (Supplemental Figure 1B). The α7 protein detected in this Blot is an aggregation with a molecular weight >220 kDa; the expected molecular weight of an α7 pentamer is 280 kDa.

Labeling of A7R3HC10 *cells with alexa488-conjugated α-btx*

Intact cells were labeled with Alexa488-conjugated α-btx to qualitatively verify surface expression of α7 nAChR and to illustrate the distribution of receptor expression in this cell line. As expected, the untransfected HEK 293, HEK-hα7, and A7R3HC10 cell lines were not labeled with the fluorescent toxin. In contrast, the A7R3HC10 cell line was labeled by the fluorescent α-btx, and in a competitive manner with 1 mM nicotine (Supplemental Figure 2). The labeling appears in non-continuous clusters, suggesting that surface expression of α7 in this cell line may be non-uniform. Similar non-continuous patterns of labeling by fluorescent dye-conjugated ligands of α7 have been seen in other cell lines and in cultured neurons (Hone et al., 2010; Valles et al., 2009).

MLA sensitive α7-mediated currents in A7R3HC10 cells

The ACh-evoked responses recorded from A7R3HC10 cells with patch-clamp electrophysiology were sensitive to inhibition by the α7-selective antagonist MLA in a concentration-dependent manner (Supplemental Figure 3). In this experiment, the ACh concentration was fixed at 170 μM (the EC_{50} for peak currents), with increasing co-applications of MLA. No pre-incubation with MLA was made in these experiments. The IC_{50} of MLA measured in this paradigm was 2.7±0.4 μM. Since chronic applications of MLA are often made at nanomolar concentrations to produce selective inhibition of a7 receptors, this may seem like a rather high value for MLA, but when one considers that IC_{50} values are dependent on variables such as agonist concentration, timing, and duration of antagonist applications, this value is reasonable. High affinity inhibition of α7-mediated responses is obtained only when MLA is pre-incubated prior to the application of agonist (Alkondon, 1992; Palma et al., 1996). In addition, the IC_{50} value of MLA in an oocyte experiment utilizing a similar protocol to the one used here (no MLA pre-incubation) was determined to be 1.2 ± 0.2 μM with an ACh concentration of 60 μM (Lopez-Hernandez et al., 2009). Given that the ACh concentration used here was 170

μM, or roughly 3-fold higher, the IC_{50} of 2.7±0.4 μM for MLA inhibition of responses evoked by 170 μM ACh is consistent with previously published data.

Calculation of the drug dilution factor for the pressure-application system

Drug solutions applied via the picospritzer system were previously determined to be diluted approximately 30-fold in experiments with hippocampal brain slices (Lopez-Hernandez et al., 2007). In this study, the picospritzer system was used in a similar manner to apply drugs, with the exception that drugs were applied to cultured cells rather than brain slices. In order to determine the effective dilution factor of drugs delivered to the cultured cells via picospritzer, shifts in the transmembrane potential were recorded by current-clamp as solutions with varying K^+ concentrations were applied to the cell. The shift in transmembrane potential was first determined when an external solution containing 50 mM K^+ was applied via bath perfusion. Then, test solutions containing various K^+ concentrations were applied to the cells via picospritzer, and comparisons were made to determine which concentration of K^+ applied via the picospritizer shifted the transmembrane potential most similarly to that observed when 50 mM K^+ was bath-perfused. Differences in osmolarity between experimental solutions were minimized by the addition of sucrose. The magnitude of the observed shift in transmembrane potential upon application of experimental K^+ solutions was dependent on the initial resting membrane of a cell; cells with resting potentials further away from the new equilibrium potential of K^+ showed larger shifts. As shown in Supplemental Figure 4, the relationship between resting membrane potential and depolarization was linear for a given K^+ concentration. The close correspondence between the 75 mM K^+ concentration in the drug delivery pipette and the 50 mM K^+ concentration delivered in the bath indicates that the effective dilution factor of solution applied via picospritzer in this study was 1.5. The dilution factor to cultured cells was expected to be smaller than with brain slices as the applied drug has to penetrate extracellular matrix/tissue layers to reach the neurons expressing the receptor of interest in brain slices. Based on this result, drug solutions were prepared that were 1.5-fold more concentrated than the desired final concentration when the picospritzer system was used. For example, 1.5 mM ACh was placed in the drug application pipette when 1 mM ACh was desired to be applied to the cell.

Apparent temperature-dependence of alpha7 positive allosteric modulators from whole-cell recordings

Although *in vivo* data with α7 PAMs are limited, the data that are available show that α7 PAMs produce effects when administered to living animals, suggesting that α7 PAMs work at physiological temperatures (reviewed in (Williams et al., 2011)). However, it has recently been reported that the potentiation of responses by the α7 PAMs PNU-120596 and SB-206553 may have a dependence on the temperature, with potentiation being drastically reduced near physiological temperatures (Sitzia et al., 2011). To investigate the effect of temperature on α7 PAM efficacy, we tested the activities of type I and type II PAMs at 37 ºC with whole-cell recordings from the HEK-hα7/hric3 cell line. The basic protocol used in these experiments was to obtain three responses at room temperature (23.5 °C), record three responses at 37 °C, and then reduce the temperature back down to 23.5 °C. Acetylcholine was co-applied with PAM for 3 seconds with 60-second inter-stimulus intervals. It is important to note that at 37 ºC the quality of the whole-cell seals usually decreased. Because of this, the parameters used to define an acceptable whole-cell recording at 37 ºC were more relaxed than they would be for a typical whole-cell recording made at room temperature. Whole-cell seals with access resistance <40 MΩ, input resistance >100 MΩ, and holding current <700 pA at 37 °C were included in the analysis. Prior to the increase in temperature, access resistances were <15 MΩ, input resistances were >1 GΩ, and the holding current was between -50 pA and 0 pA. In most cases, if the patch survived the time at 37 ºC, the whole-cell parameters improved as temperatures returned to room temperature. In rundown control experiments performed without temperature adjustments, the amplitude of the responses at the end of the experiment were ~70% of the responses at the beginning (Figure 6A-B).

When 1 mM ACh was applied without a PAM, peak currents at 37 °C were 47 ± 3% of the initial baseline currents recorded at 23.5 °C and they recovered to ~80% upon temperature reduction back to 23.5 °C, a full recovery based on the rundown control (Supplemental Figure 5C-D and Table 2). It is important to emphasize that in these experiments currents evoked by ACh alone were reduced by approximately 53% at 37 °C relative to 23.5 °C because when evaluating the effect of temperature on PAM potentiation the ACh-evoked responses recorded at 37 °C are used as the baseline for comparison. This observation confirms recent findings that responses evoked by ACh on α7 nAChR are reduced at 37 °C relative to room temperature (Jindrichova et al., 2012; Sitzia et al., 2011).

The potentiation of responses evoked by 100 μM ACh with either 1 mM 5-HI or 10 μM NS-1738, (both type I PAMs) at 37 °C was similar (Figure 7 and Table 2). With 1 mM 5HI potentiated responses were 33 ± 2% (67% reduction) and with 10 μM NS-1738

potentiated responses were 34 ± 5% (66% reduction) of the baseline responses at room temperature, both of which were significantly smaller than the reduction seen with ACh alone ($p<0.05$). In both cases the potentiated responses recovered when temperatures returned to 23.5 °C to an extent expected (~70-80%) based on the rundown control. Together, these results suggest that the ability of the type I PAMs to potentiate ACh-evoked responses may be reduced, but relatively conserved at physiological temperature.

Legends for Supplemental Figures

Supplemental Figure 1. Expression of human α7 and human RIC-3 by the A7R3HC10 cell line. A) Expression of hα7 and hRIC-3 mRNA is verified by RT-PCR. The observed bands for GAPDH, hα7, and hRIC-3 are 516 bp, 414 bp, and 346 bp, as expected for the primers used. B) Immunoprecipitation and western blot from cell lysates. Untransfected HEK 293 and hRIC-3 cells were negative for hα7 protein with hα7-alone cells being slightly positive, and A7R3HC10 cells being strongly positive. The labeled protein from HEK-hα7 and A7R3HC10 cell lysates is an aggregate with molecular weight > 220 kDa. The primary antibodies for α7 were generously provided by Dr. Cecilia Gotti (University of Milan, Italy).

Supplemental Figure 2. Labeling of intact A7R3HC10 cells with Alexa Fluor 488-α-btx. No labeling was observed for untransfected HEK 293, HEK-hRIC-3, or HEK-hα7 cell lines. In contrast, labeling was observed on A7R3HC10 cells in a competitive manner with 1 mM nicotine. Cellular nuclei are stained in blue with DAPI, and the Alexa Fluor 488-α-btx label is green.

Supplemental Figure 3. Inhibition of currents by MLA from A7R3HC10 cells. Inhibition of responses by MLA determined from peak responses. In these experiments increasing MLA concentrations were co-applied with 170 μM ACh, the EC_{50} for peak currents determined previously (Figure 1B). A) Each point represents the mean ± SEM determined from 4-6 cells. The holding potential was -70 mV. B) Representative traces illustrating the co-applied inhibition at varying concentrations of MLA compared to the control responses to 170 μM ACh.

Supplemental Figure 4. Determination of dilution factor in the pressure drug application system with cultured cells. Whole-cell current-clamp recordings were carried out while applying solutions containing various concentrations of KCl to A7R3HC10

cells. The relationship between the initial resting membrane potential and depolarization was linear for a given K^+ concentration (left panel). Shifts in the transmembrane potential when applying 75 mM KCl via picospritzer is most similar to those observed when applying 50 mM KCl via bath perfusion (right panel), suggesting that the dilution factor of the pressure application drug delivery system with cultured cells was 1.5.

Supplemental Figure 5. Agonist controls for whole-cell voltage-clamp recordings investigating the temperature effects of α7 PAMs. A & B) Rundown control performed at room temperature (n=15). A) Responses to the 3-second application of 1 mM ACh were recorded every 60 seconds and normalized to the maximum peak amplitude of each cell (black circles). B) Representative traces. C & D) Temperature-dependent effects of peak responses evoked by 1 mM ACh (n=7). C) Responses were normalized to the average peak amplitude recorded at 23.5 °C. Each data point is shown as the average normalized value ± SEM (black circles). Temperature is indicated by gray squares. D) Representative traces.

Supplemental Figure 6. Temperature dependence of alternative PAMs on potentiation of α7-mediated responses. Whole-cell currents from A7R3HC10 cells evoked by 3 second co-applications of ACh and PAM were recorded every 60 seconds with varied temperatures between 23.5 °C and 37 °C. A) Time course for 100 μM ACh and 1 mM 5-HI evoked peak responses (black circles, n=12). Temperature is indicated by gray squares. B) Representative traces of 100 μM ACh and 1 mM 5-HI evoked responses recorded at the indicated temperature. C) Time course for 100 μM ACh and 10 μM NS-1738 evoked peak responses (black circles, n=6). Temperature is indicated by gray squares. D) Representative traces of 100 μM ACh and 10 μM NS-1738 evoked responses recorded at the indicated temperature. Responses were normalized to the average peak amplitude of the three initial responses obtained at 23.5 °C. Each data point was represented as the average normalized value ± SEM. E) Time course for 100 μM ACh and 10 μM TQS evoked peak responses (black circles, n=7). Temperature is indicated by gray squares. F) Representative traces of 100 μM ACh and 10 μM TQS evoked responses recorded at the indicated temperature. The deterioration in whole-cell recording properties at 37 °C could lead to a reduction in the fidelity of the voltage-clamp. It is feasible that the currents evoked in the presence of PNU-120596, given their size, could contribute to a greater loss of voltage-clamp fidelity than may have occurred with ACh alone. However, the increased temperature had less effect on the responses evoked with TQS than on the responses evoked with PNU-120596, relative to their initial

baseline responses (46 ± 3% versus 12 ± 3%), despite the fact that the absolute magnitude of the responses recorded with TQS was larger than those with PNU-120596 (3,080 ± 484 pA versus 1,333 ± 414 pA at 23.5 °C and 1,438 ± 229 pA versus 104 ± 31 pA at 37 °C).

Supplemental References

Alkondon M, Pereira, E.F.R., Wonnacott, S., and Albuquerque, E.X. (1992) Blockade of nicotinic currents in hippocampal neurons defines methyllycaconitine as a potent and specific receptor antagonist. *Mol Pharmacol* **41**:802-808.

Hone AJ, Whiteaker P, Mohn JL, Jacob MH and McIntosh JM (2010) Alexa Fluor 546-ArIB[V11L;V16A] is a potent ligand for selectively labeling alpha 7 nicotinic acetylcholine receptors. *J Neurochem* **114**(4):994-1006.

Jindrichova M, Lansdell SJ and Millar NS (2012) Changes in temperature have opposing effects on current amplitude in alpha7 and alpha4beta2 nicotinic acetylcholine receptors. *PLoS One* **7**(2):e32073.

Lopez-Hernandez G, Placzek AN, Thinschmidt JS, Lestage P, Trocme-Thibierge C, Morain P and Papke RL (2007) Partial agonist and neuromodulatory activity of S 24795 for alpha7 nAChR responses of hippocampal interneurons. *Neuropharmacology* **53**(1):134-144.

Lopez-Hernandez GY, Thinschmidt JS, Zheng G, Zhang Z, Crooks PA, Dwoskin LP and Papke RL (2009) Selective inhibition of acetylcholine-evoked responses of alpha7 neuronal nicotinic acetylcholine receptors by novel tris- and tetrakis-azaaromatic quaternary ammonium antagonists. *Mol Pharmacol* **76**(3):652-666.

Palma E, Bertrand S, Binzoni T and Bertrand D (1996) Neuronal nicotinic alpha 7 receptor expressed in Xenopus oocytes presents five putative binding sites for methyllycaconitine. *J Physiol* **491**:151-161.

Sitzia F, Brown JT, Randall AD and Dunlop J (2011) Voltage- and Temperature-Dependent Allosteric Modulation of alpha7 Nicotinic Receptors by PNU120596. *Front Pharmacol* **2**:81.

Valles AS, Roccamo AM and Barrantes FJ (2009) Ric-3 chaperone-mediated stable cell-surface expression of the neuronal alpha7 nicotinic acetylcholine receptor in mammalian cells. *Acta Pharmacol Sin* **30**(6):818-827.

Williams DK, Wang J and Papke RL (2011) Positive allosteric modulators as an approach to nicotinic acetylcholine receptor-targeted therapeutics: Advantages and limitations. *Biochem Pharmacol* **82**(8):915-930.

Supplemental Figures

Figure S1

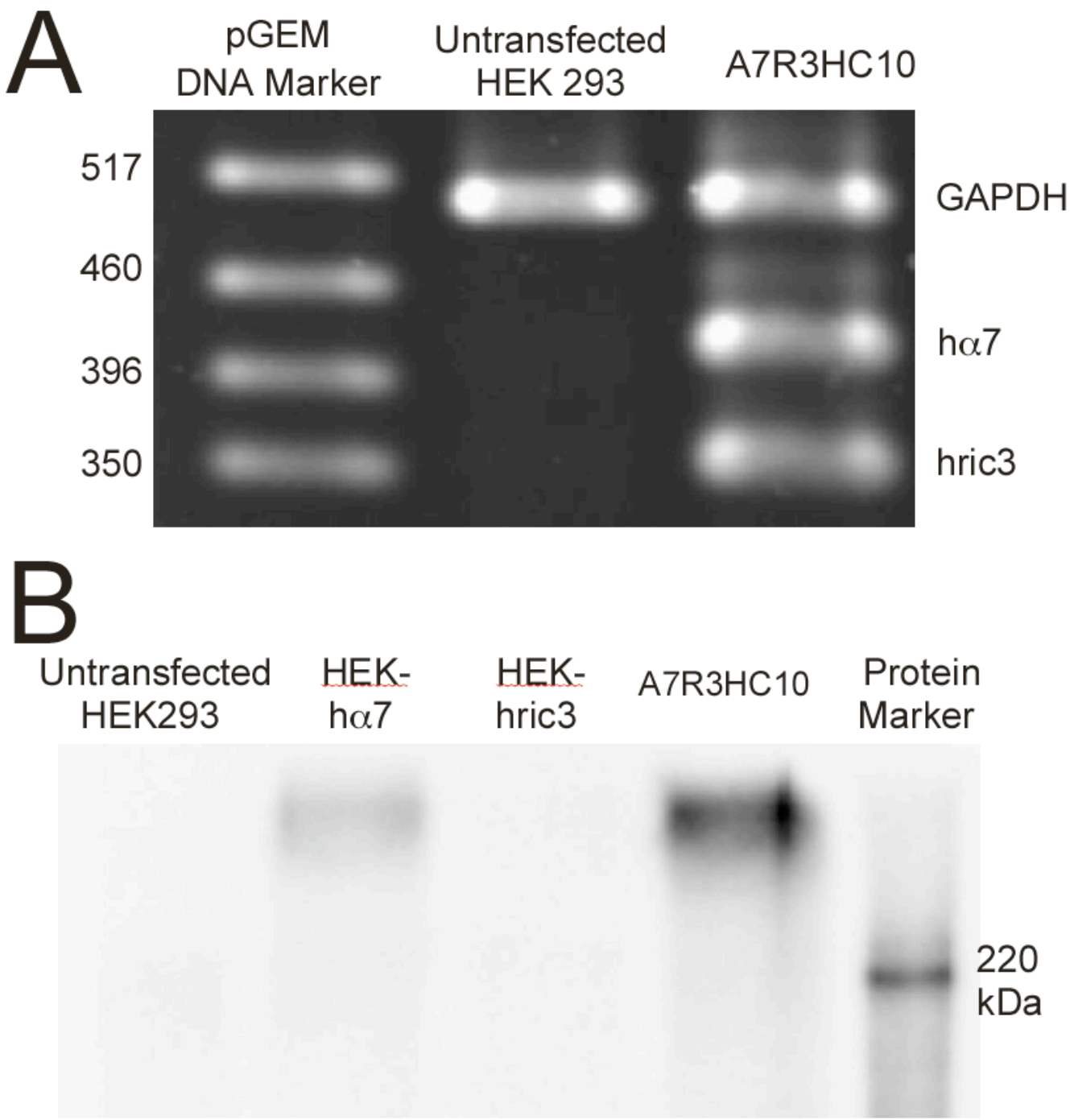
A
pGEM
DNA Marker
Untransfected
HEK 293
A7R3HC10
517
460
396
350
GAPDH
hα7
hric3
B
Untransfected
HEK293
HEK-
hα7
HEK-
hric3
A7R3HC10
Protein
Marker
220
kDa

Figure S2

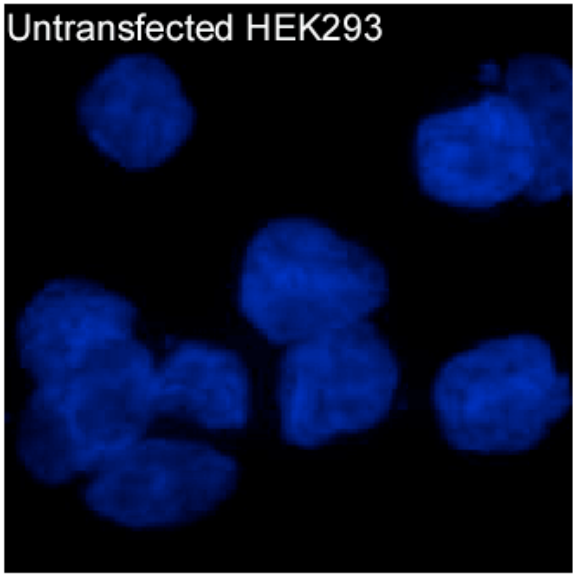
Untransfected HEK293

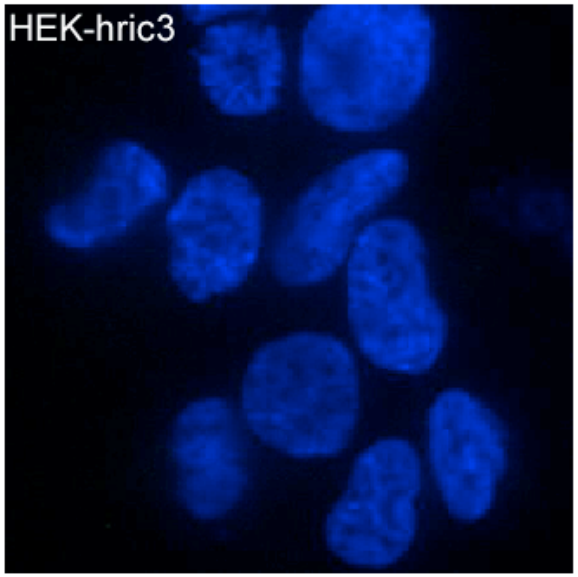
HEK-hric3

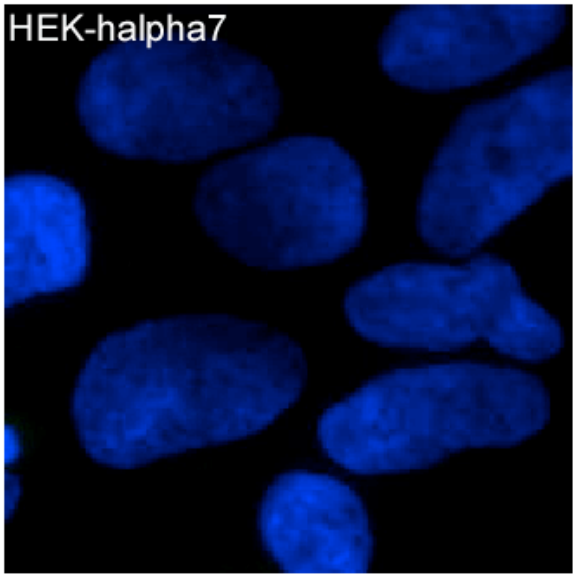
HEK-halpha7

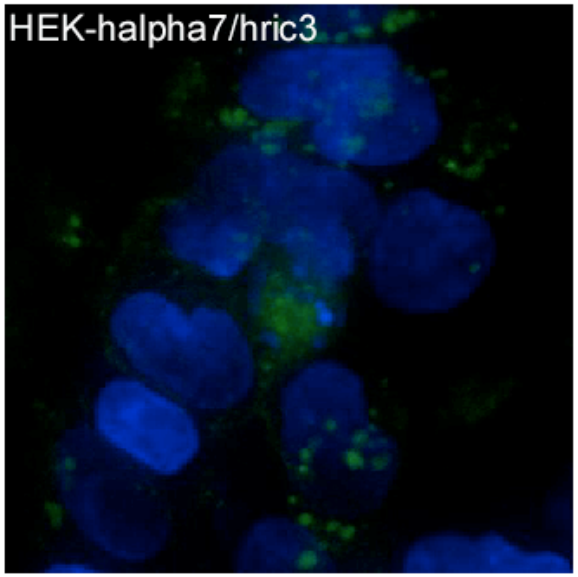
HEK-halpha7/hric3

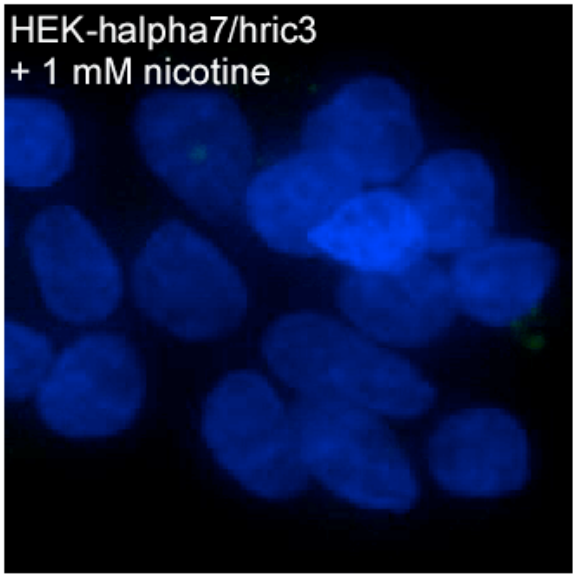
HEK-halpha7/hric3
+ 1 mM nicotine

A

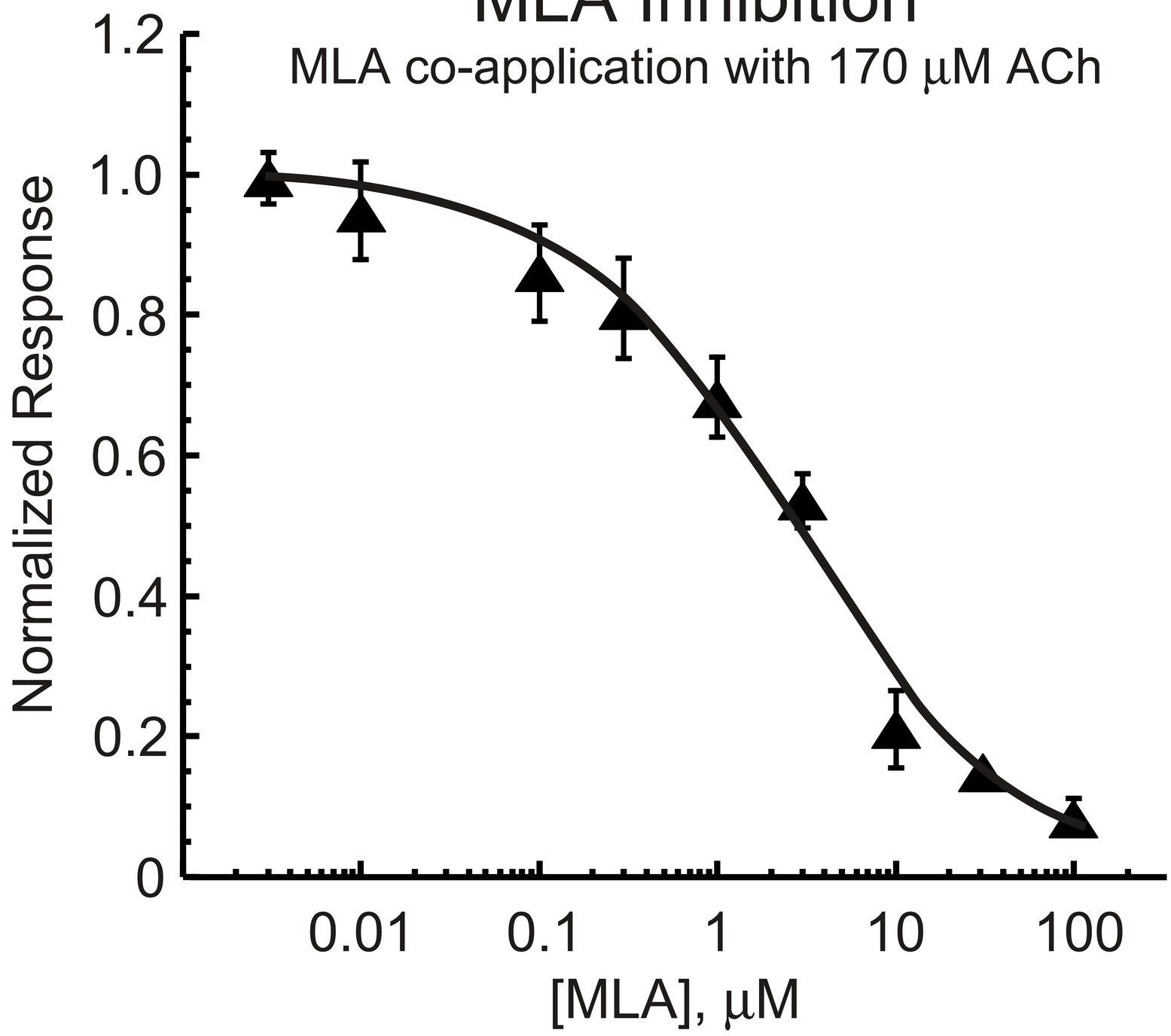
MLA Inhibition
MLA co-application with 170 μM ACh
Normalized Response
1.2
1.0
0.8
0.6
0.4
0.2
0
0.01
0.1
1
10
100
[MLA], μM

B

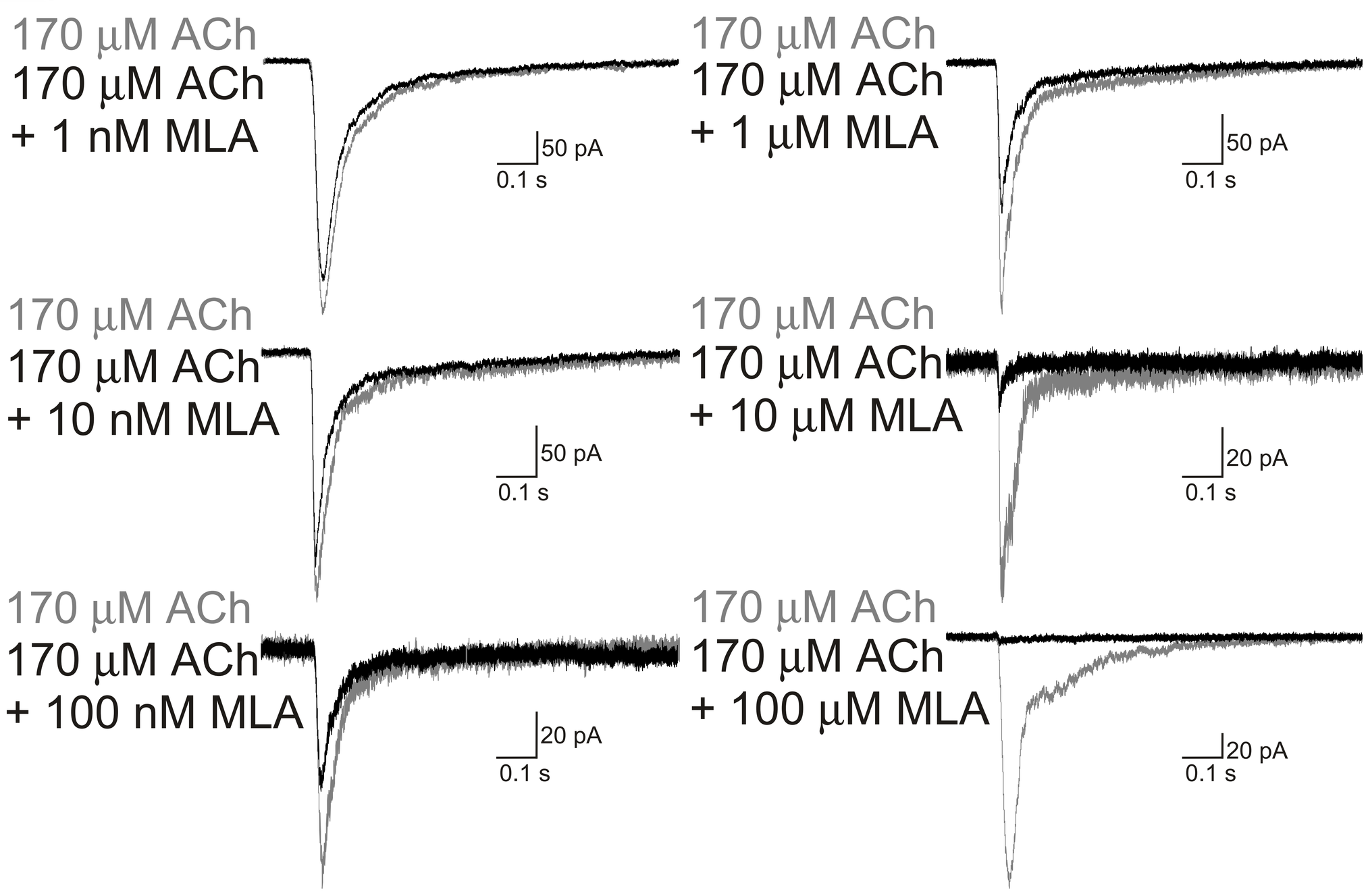
170 μM ACh
170 μM ACh
+ 1 nM MLA
50 pA
0.1 s
170 μM ACh
170 μM ACh
+ 1 μM MLA
50 pA
0.1 s
170 μM ACh
170 μM ACh
+ 10 nM MLA
50 pA
0.1 s
170 μM ACh
170 μM ACh
+ 10 μM MLA
20 pA
0.1 s
170 μM ACh
170 μM ACh
+ 100 nM MLA
20 pA
0.1 s
170 μM ACh
170 μM ACh
+ 100 μM MLA
20 pA
0.1 s

Figure 3S

Figure S4

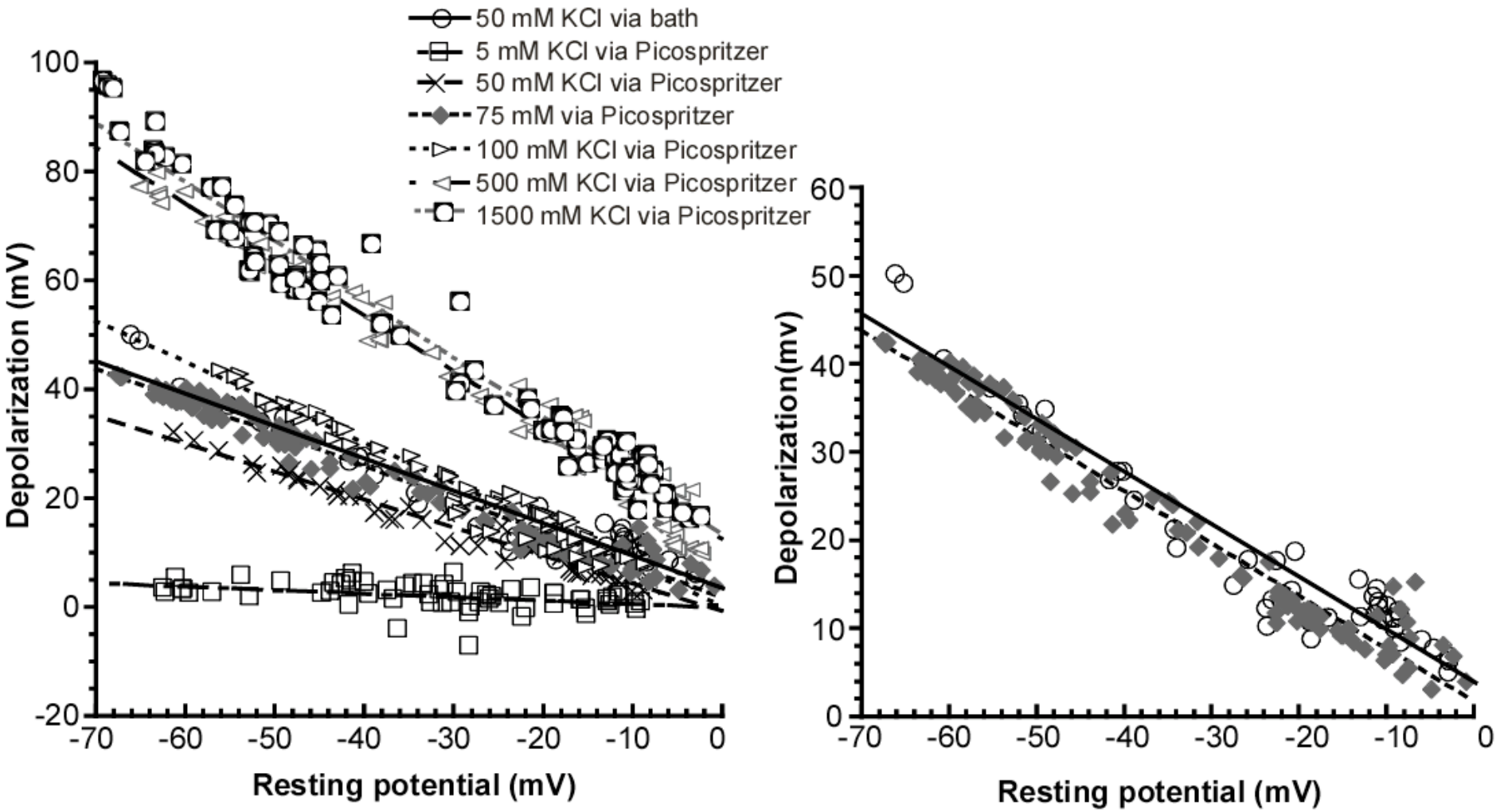
50 mM KCl via bath
5 mM KCl via Picospritzer
50 mM KCl via Picospritzer
75 mM via Picospritzer
100 mM KCl via Picospritzer
500 mM KCl via Picospritzer
1500 mM KCl via Picospritzer
Depolarization (mV)
Resting potential (mV)
Depolarization(mv)
Resting potential (mV)

Figure S5

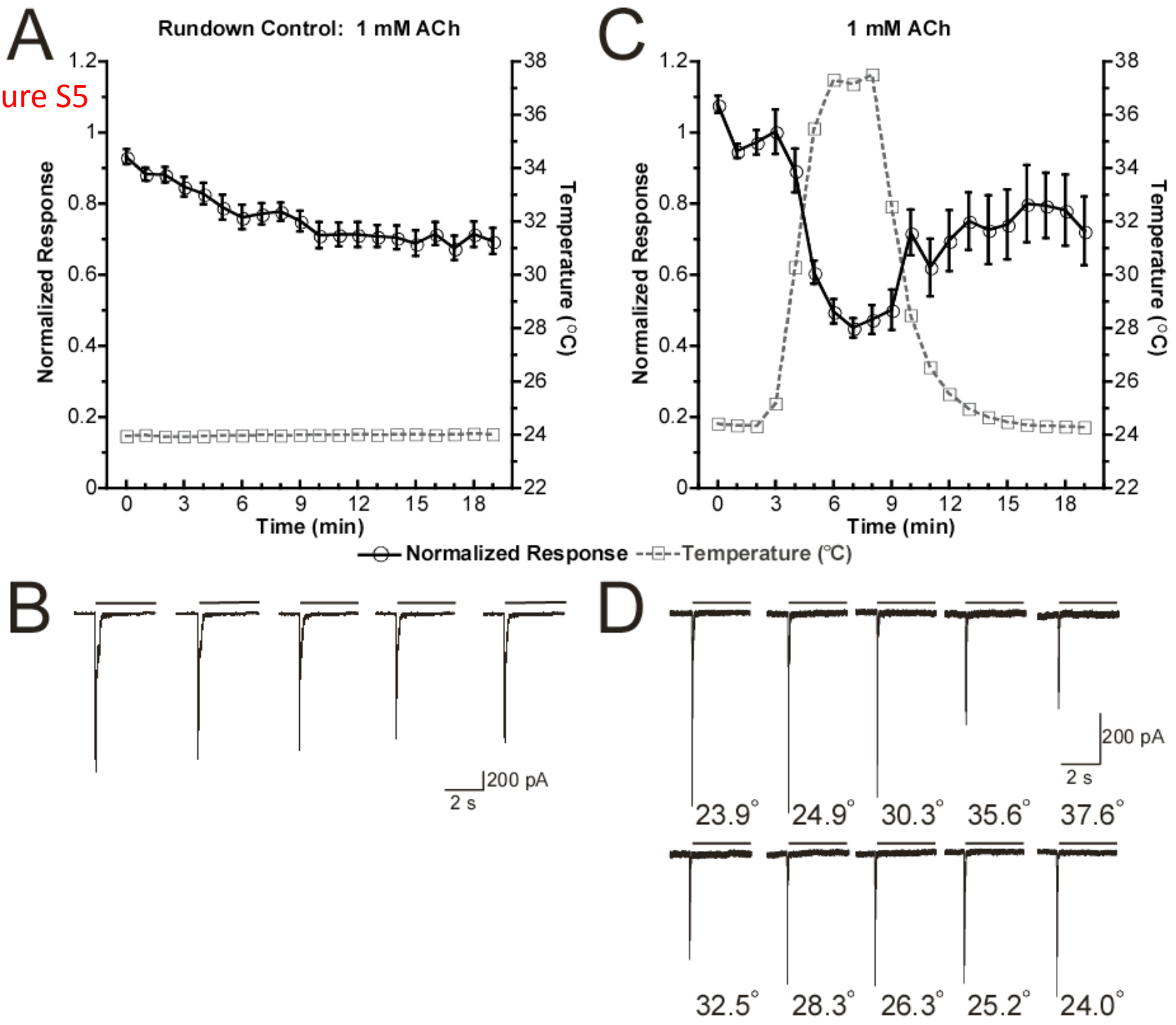
A
Rundown Control: 1 mM ACh
Normalized Response
Temperature (°C)
Time (min)
C
1 mM ACh
Normalized Response
Temperature (°C)
Time (min)
Normalized Response
Temperature (°C)
B
200 pA
2 s
D
200 pA
2 s
23.9°
24.9°
30.3°
35.6°
37.6°
32.5°
28.3°
26.3°
25.2°
24.0°

Figure S6

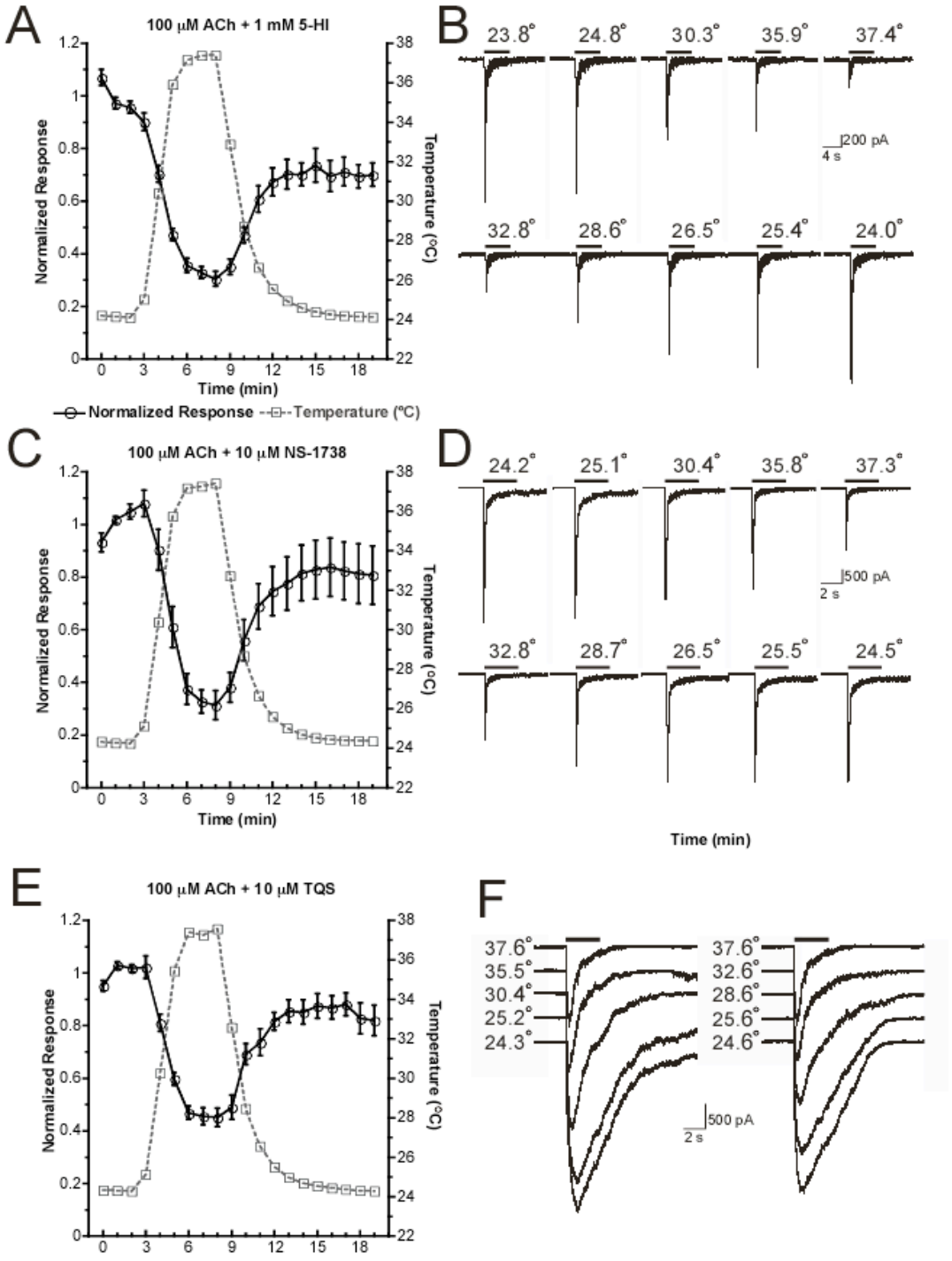
A
100 μM ACh + 1 mM 5-HI
Normalized Response
Temperature (°C)
Time (min)
Normalized Response
Temperature (°C)
B
23.8°
24.8°
30.3°
35.9°
37.4°
200 pA
4 s
32.8°
28.6°
26.5°
25.4°
24.0°
C
100 μM ACh + 10 μM NS-1738
Normalized Response
Temperature (°C)
Time (min)
D
24.2°
25.1°
30.4°
35.8°
37.3°
500 pA
2 s
32.8°
28.7°
26.5°
25.5°
24.5°
Time (min)
E
100 μM ACh + 10 μM TQS
Normalized Response
Temperature (°C)
F
37.6°
35.5°
30.4°
25.2°
24.3°
37.6°
32.6°
28.6°
25.6°
24.6°
500 pA
2 s